

Interaction Note

Note 616

April 2011

**Lightning Induced Waveforms 4 and 5A in Composite Airframes,  
The Inability of Copper Braid to Shield It,  
and  
A New Layered Copper Braid and High-mu Foil Shield**

Interaction Note 608 Revision A

Larry West  
10215 Beechnut St., Suite 1003  
Houston, TX 77072

*abstract, Rev A*

IN615 shows that Waveform 5A is the result of system level ground-tests with a nearby return current. In-flight, there is no return current. The ground-test therefore creates the external inductance between the aircraft currents and the return current. In-flight, the common mode currents are subject only to the internal inductance of the conductors which is two orders of magnitude smaller than the ground-test external inductance. The result is that Waveform 5A (WF5A) ground-test cable current becomes Waveform 4 (WF4) cable current in-flight. The shielding problem remains the same as does the solution since WF5A is the late time part of WF4. The only changes herein are the numerics in changing from Waveform 5A to Waveform 4 along with minor editing for clarity. It was written for those who do not believe that lightning currents penetrate normal copper shields.

*abstract, Rev 0*

A simple theory is presented of how lightning induced Waveform 5 currents appears on cables in composite airframes and why it does not rise as fast as the lightning pulse or as slow as the RL time constant of the cable. Why normal copper braid shields do not work against it is explained using Schelkunoff's theory of coaxial cable shields. A new cable shield design using layers of copper and high-mu foil is developed that will protect against Waveform 5 currents and not saturate. The effects of the new cable shield on signals passing through it are discussed. Finally, a lab test is designed for verifying the models.

# 1. INTRODUCTION

This paper takes IN608<sup>27</sup> further based upon the conclusions of IN617<sup>23</sup> with (1) a simple theory of how the low frequency Waveform 5A (WF5A) induced lightning current (23μs rise time and 79μs decay time)<sup>4</sup> develops on cables in composite airframes during ground testing where a return current is nearby, (2) why that current waveform changes to WF4 (1.5μs rise and 88μs decay) in-flight because there is no return current, (3) why normal copper braid cable shields do not attenuate the low frequencies, and (4) a new cable shield design<sup>21</sup> for protecting electrical and electronic systems from this little understood phenomenon. This revision reflects more detailed analysis following IN615.

Following up, the above lightning interaction applies only to the system level ground-test with a nearby return current creating an external inductance between the differential mode currents. In-flight, there is no return current and the inductance of the common mode cable currents is the internal inductance. For a conducting cylinder of length,  $l$ , radius,  $R$ , thickness,  $t$ , permeability,  $\mu$ , and conductivity,  $\sigma$ , the low frequency ( $\omega \cdot \tau_d = \omega \cdot \mu \cdot \sigma \cdot t^2 < 1$ ) internal inductance is as follows:<sup>1</sup>

$$(1) \quad L_{int} = \frac{\mu_0 \cdot l}{4 \cdot \pi} \cdot \frac{t}{R}$$

The high frequency ( $\omega \cdot \tau_d = \omega \cdot \mu \cdot \sigma \cdot t^2 \geq 1$ ) internal inductance is as follows:

$$(2) \quad L_{int} = \frac{\mu_0 \cdot l}{4 \cdot \pi} \cdot \frac{\delta}{R} \text{ where } \delta = \sqrt{1/\pi \cdot f \cdot \mu \cdot \sigma} \text{ is the skin depth.}$$

Composite airframes exposed to direct strike lightning with a 200kA Component A current will have as much as ten thousand volts built up along the airframe and between boxes in the airframe. A notional picture of a composite cylindrical airframe with a shielded cable is shown in Figure 1. A 1kΩ lightning source impedance would be acceptable to the phenomenologists but it is unnecessary for this modeling because it is much larger than the loads.

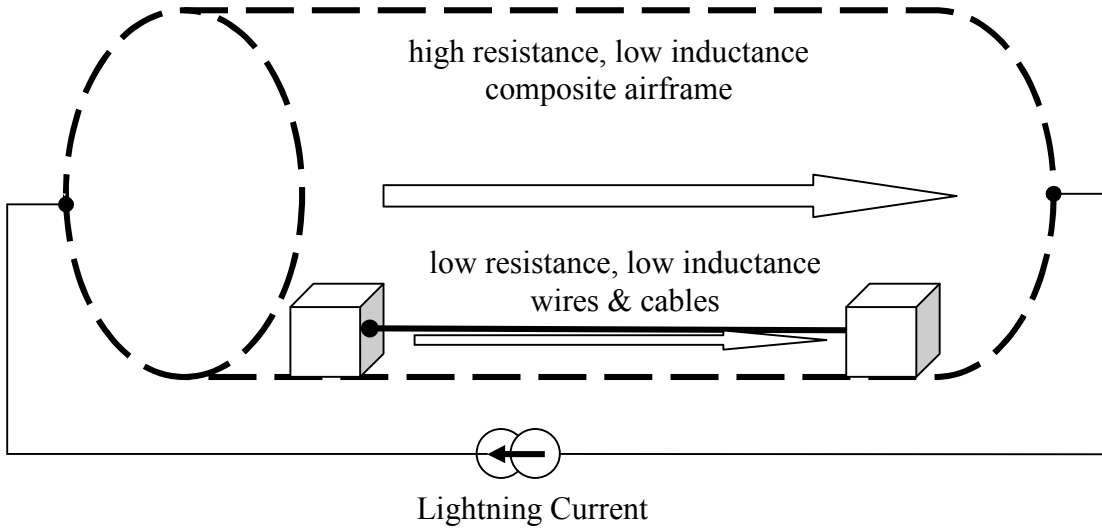


**Figure 1. Composite Airframe with Shielded Cable/Wire (Revised to In-Flight)**

The external inductance of the cylinder in a coaxial ground-test fixture is as follows:

$$(3) \quad L_{ext} = \frac{\mu_0 \cdot l}{2 \cdot \pi} \cdot \ln\left(\frac{R_{fixture}}{R_{cylinder}}\right)$$

The internal inductance of a 10m long cylinder with a radius of 1m and skin thickness 2mm is  $L_{int} = 6nH$  while the external inductance in the coaxial fixture with the return current conductors twice the cylinder radius is  $L_{ext} = 436nH$ . That difference causes the induced cable currents to change from Waveform 5A in the ground-test to Waveform 4 in-flight as will be shown below.

The problem is exacerbated when the skin depth of the cable shields is equal to or greater than the shields' thickness and the separation of the external and shielded internal regions disappears.

This note treats the problem of induced lightning currents on the cable shields so low in frequency that the skin depth is greater than the copper cable shield thickness using Schelkunoff's 74 year old theory.<sup>1</sup> A new cable shield design is then developed using layers of copper braid and high- $\mu$  foil. Note that throughout, the boxes' thickness is assumed to be large compared to that of the cable shield and the box's skin depth.

This revision simply replaces Waveform 5A cable current with Waveform 4, both defined as follows:<sup>6</sup>

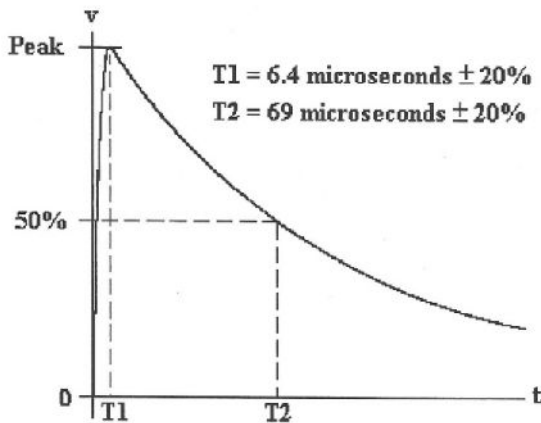


Figure 2.a<sup>6,4</sup>. Waveform 4

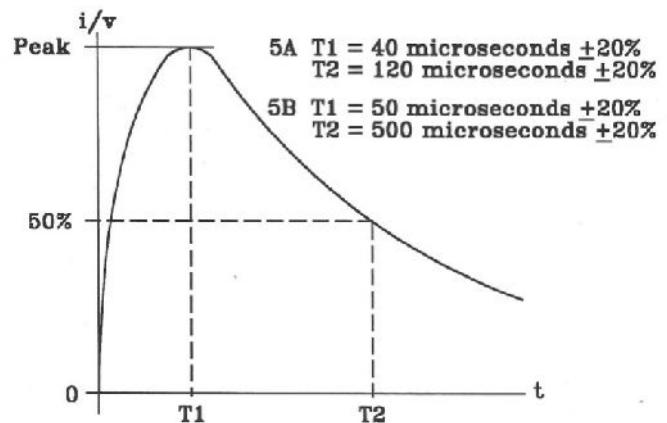


Figure 2.b<sup>6,4</sup>. Waveforms 5A & 5B

From reference 6, WF5A and WF4 are defined as the following:

$$(4) \quad I_{WF5A}(t) \equiv I_{5A} \cdot 2.334 \cdot (e^{-t/79\mu s} - e^{-t/23\mu s}), \text{ time-to-peak} = 40\mu s, \text{ and}$$

$$(5) \quad I_{WF4}(t) \equiv I_4 \cdot 1.094 \cdot (e^{-t/88\mu s} - e^{-t/1.5\mu s}), \text{ time-to-peak} = 6.4\mu s,$$

where the time-to-peak is the same as the standards in Figures 2.a and 2.b, above. The multipliers are necessary to obtain the correct peak values for the double exponential waveforms.

-----  
 The author would like to thank the following people for many conversations about this elusive little investigated subject that affects every composite vehicle: J. A. (Andy) Plumer, Tom Pierce, Roxanne Arellano, Jim Lambert, Bob Scully, Carl E. Baum, and John Norgard.

## 2. SIMPLE LOW FREQUENCY CIRCUIT MODEL FOR CURRENT DIVISION

A simple heuristic circuit model of Figure 1 follows:<sup>27</sup>

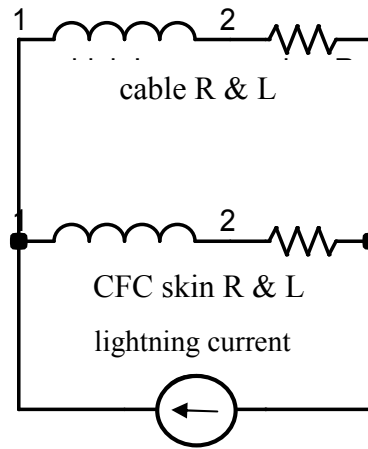


**Figure 3. Heuristic Circuit Model for Lightning Current Division in a Composite Airframe**

As a notional example, we will use a 100mΩ, 500nH, composite skin and a 20mΩ, 3μH, internal braid for ground test parameters and 4nH CFC skin and 25nH cable shield for in-flight parameters. The driving current is the SAE ARP5412A Component A.

The lightning strike Component A is as follows in the time domain:

$$(1) \quad I(t) = I_A \cdot (e^{-a \cdot t} - e^{-b \cdot t}), \text{ where}$$

$$b = 647,265 \text{ sec}^{-1} = 1/1.5\mu\text{s},$$

$$a = 11,354 \text{ sec}^{-1} = 1/88\mu\text{s}, \text{ and}$$

$I_A$  is 218,810 amps, which gives the peak double exponential amplitude of 200kA.

The Laplace transform of the lightning waveform is as follows:

$$(2) \quad I(s) = 218kA \cdot \left( \frac{1}{s+a} - \frac{1}{s+b} \right)$$

The voltage across the system is as follows:

$$(3) \quad V(s) = I(s) \cdot Z(s)$$

where  $Z(s)$  is impedance of the two parallel branches:

$$(4) \quad Z(s) = \left( \frac{1}{R_{CFC} + s \cdot L_{CFC}} + \frac{1}{R_{braid} + L_{braid} \cdot s} \right)^{-1} = \frac{L_{CFC} \cdot L_{braid}}{L_{CFC} + L_{braid}} \cdot \frac{(s+a) \cdot (s+b)}{s+\gamma}$$

where

$L_{braid}$  is the braid inductance, 3μH ground-test, 25nH in-flight,  
 $L_{CFC}$  is the composite (CFC) skin inductance, 500nH ground-test, 4nH in-flight,  
 $R_{braid} = 20\text{m}\Omega$ ,  
 $R_{CFC} = 100\text{m}\Omega$ ,  
 $\alpha = R_{braid}/L_{braid} = 1/150\mu\text{s}$  ground-test, 1/1.3μs, in-flight,  
 $\beta = R_{CFC}/L_{CFC} = 1/5\mu\text{s}$  ground-test, 1/40ns in-flight,  
 $\gamma = (R_{braid}+R_{CFC})/(L_{braid}+L_{CFC}) = 1/29\mu\text{s}$  ground test, 1/250ns in-flight, the loop inverse time constant.

The current through the CFC and the braid in the frequency domain are as follows:

$$(5) \quad I_{CFC}(s) = \frac{V(s)}{Z(s)} = I_A \cdot \frac{L_{braid}}{L_{CFC} + L_{braid}} \cdot \left( \frac{1}{s+\alpha} - \frac{1}{s+\beta} \right) \cdot \frac{s+\alpha}{s+\gamma}, \text{ and}$$

$$(6) \quad I_{braid}(s) = \frac{V(s)}{Z(s)} = I_A \cdot \frac{L_{CFC}}{L_{CFC} + L_{braid}} \cdot \left( \frac{1}{s+\alpha} - \frac{1}{s+\beta} \right) \cdot \frac{s+\beta}{s+\gamma}$$

Note that the system parameter in the denominator that controls the waveshape is the loop time constant,  $\gamma^{-1}$ .

The inverse Laplace transforms of these currents are as follows:<sup>3</sup>

Currents in the composite skin are  $I_{skin} = I_{as} - I_{bs}$ , where

$$(7) \quad I_{as}(t) = I_A \cdot \frac{L_{braid}}{L_{CFC} + L_{braid}} \cdot \left\{ \frac{[\alpha^2 - a \cdot (\alpha + \beta) + \alpha \cdot \beta] \cdot e^{-\alpha \cdot t}}{(\alpha - a) \cdot (\gamma - a)} + \frac{[\gamma^2 - \gamma \cdot (\alpha + \beta) + \alpha \cdot \beta] \cdot e^{-\gamma \cdot t}}{(\alpha - \gamma) \cdot (a - \gamma)} \right\}$$

$$(8) \quad I_{bs}(t) = I_A \cdot \frac{L_{braid}}{L_{CFC} + L_{braid}} \cdot \left\{ \frac{[b^2 - b \cdot (\alpha + \beta) + \alpha \cdot \beta] \cdot e^{-b \cdot t}}{(\alpha - b) \cdot (\gamma - b)} + \frac{[\gamma^2 - \gamma \cdot (\alpha + \beta) + \alpha \cdot \beta] \cdot e^{-\gamma \cdot t}}{(\alpha - \gamma) \cdot (b - \gamma)} \right\}$$

Currents in the internal braid are  $I_{braid} = I_{ab} - I_{bb}$ , where

$$(9) \quad I_{ab}(t) = I_A \cdot \frac{L_{CFC}}{L_{CFC} + L_{braid}} \cdot \left\{ \frac{[\alpha^2 - a \cdot (\alpha + \beta) + \alpha \cdot \beta] \cdot e^{-\alpha \cdot t}}{(\alpha - a) \cdot (\gamma - a)} + \frac{[\gamma^2 - \gamma \cdot (\alpha + \beta) + \alpha \cdot \beta] \cdot e^{-\gamma \cdot t}}{(\alpha - \gamma) \cdot (a - \gamma)} \right\}$$

$$(10) \quad I_{bb}(t) = I_A \cdot \frac{L_{CFC}}{L_{CFC} + L_{braid}} \cdot \left\{ \frac{[b^2 - b \cdot (\alpha + \beta) + \alpha \cdot \beta] \cdot e^{-b \cdot t}}{(\alpha - b) \cdot (\gamma - b)} + \frac{[\gamma^2 - \gamma \cdot (\alpha + \beta) + \alpha \cdot \beta] \cdot e^{-\gamma \cdot t}}{(\alpha - \gamma) \cdot (b - \gamma)} \right\}$$

The skin and braid currents add up to the lightning current.

The resulting lightning current division between the composite skin and the braid are shown for ground-test in Figure 4a and for in-flight in Figure 4.b.

Note that in the ground-test, the early time, higher frequency, current travels through the composite skin and the late time, lower frequency, travels through the interior braid. That late time braid current is defined as Waveform 5A (WF5A) in the SAE and RTCA/DO-160 documents<sup>4, 5</sup>, that is, a rise time of 23μs and a decay time of 79μs. Note that in-flight, the currents flowing on the CFC skin and cable

shield are both Waveform 4 (WF4). That results in over 20dB more high frequency on the cables inside the aircraft than previously thought.

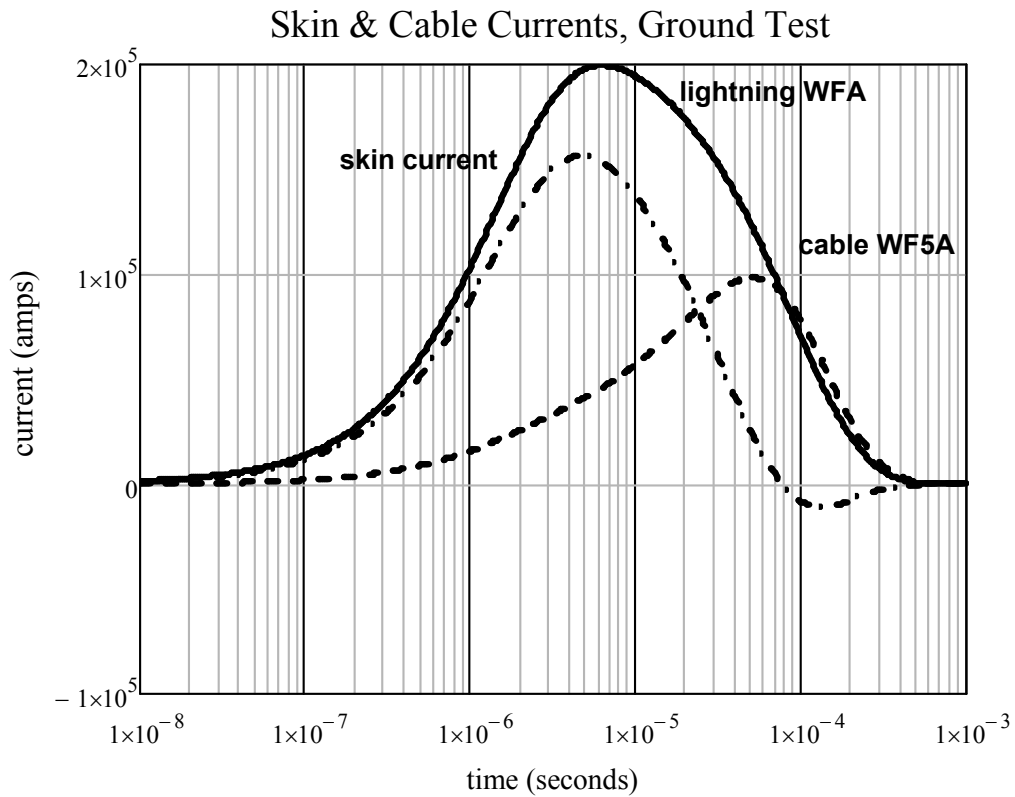


Figure 4.a. Ground-Test Current Division between Composite Skin and a Braid Cable Shield

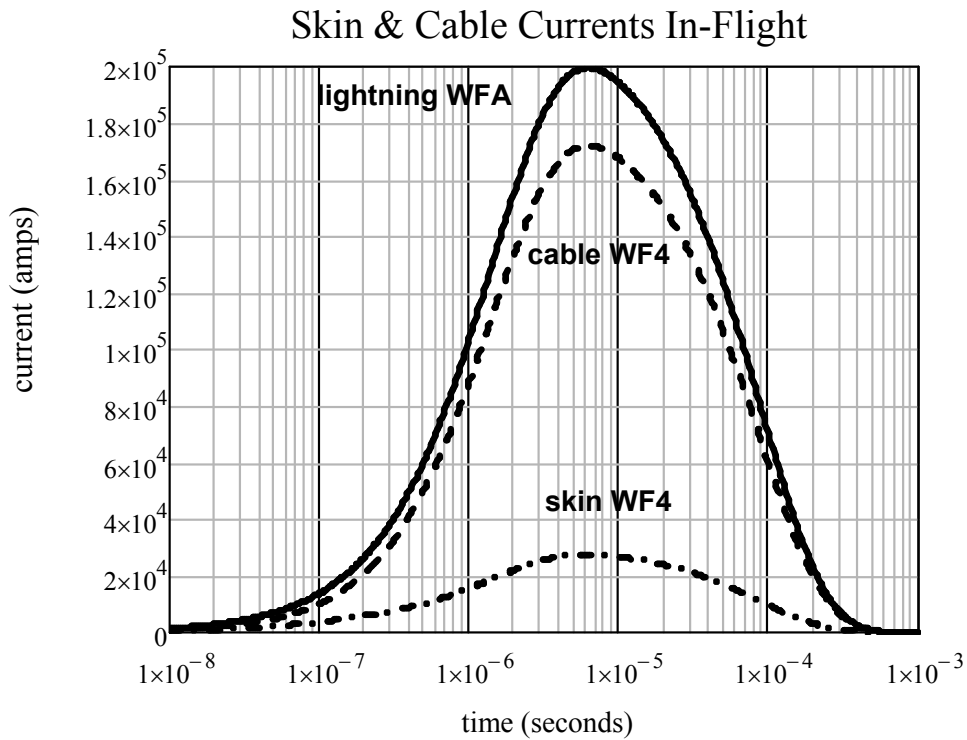
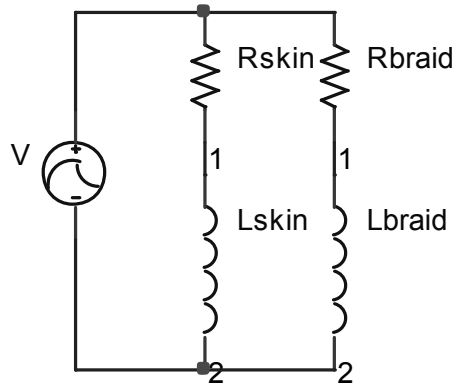


Figure 4.b. In-Flight Current Division between Composite Skin and a Braid Cable Shield

The in-flight current division is resistive while the ground-test is strongly controlled by the inductances. Note in this example that the peak braid current is 70kA (4.6dB) higher in-flight than in the ground-test and that the skin current is 130kA (14.6dB) lower.

Misunderstanding about this phenomenon exists because of what the current source imposes. Take the same two parallel RL branches driven by a notional voltage source and a notional current source in Figures 5 and 6, respectively, and see what the braid current looks like:



**Figure 5. Notional Voltage Source Driving the Parallel RL Branches**

The current through the braid branch is the following, dominated by the braid RL time constant,  $\beta^{-1}$ :

$$(11) \quad I_{braid}(s) = V(s) \cdot \frac{1}{L_{braid}(s+\beta)}$$

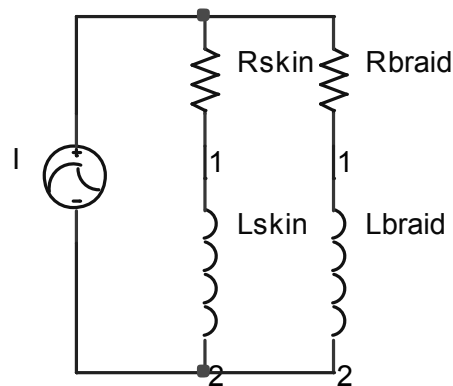


**Figure 6. Notional Current Source Driving the Parallel RL Branches**

The current through the braid branch is the following, dominated by the loop RL time constant,  $\gamma^{-1}$ :

$$(12) \quad I_{braid}(s) = I(s) \cdot \frac{L_{CFC}}{L_{CFC} + L_{braid}} \cdot \frac{s+\alpha}{s+\gamma}$$

It is the parallel paths of the two branches driven by a common current source that results in the low frequency Waveform 5A on the shield dominated by the loop time constant in ground-tests. The voltage source with the same waveform as the lightning source would induce a current on the braid that whose rise time would be dominated by the braid time constant. Therein lies the difference between conventional intuition from testing and this unique lightning phenomenon from basic theory.

### 3. COAXIAL CABLE SHIELDING

In 1934, Schelkunoff analyzed the shielding characteristics of coaxial cable shields.<sup>1</sup> Therein, solving the boundary value problem for cylindrical conductors serving as coax shields, shown in Figure 7, Schelkunoff wrote the coupled equations, 13 & 14, below, for the electric fields induced along the interior and exterior surfaces due to currents in the exterior and interior surfaces.

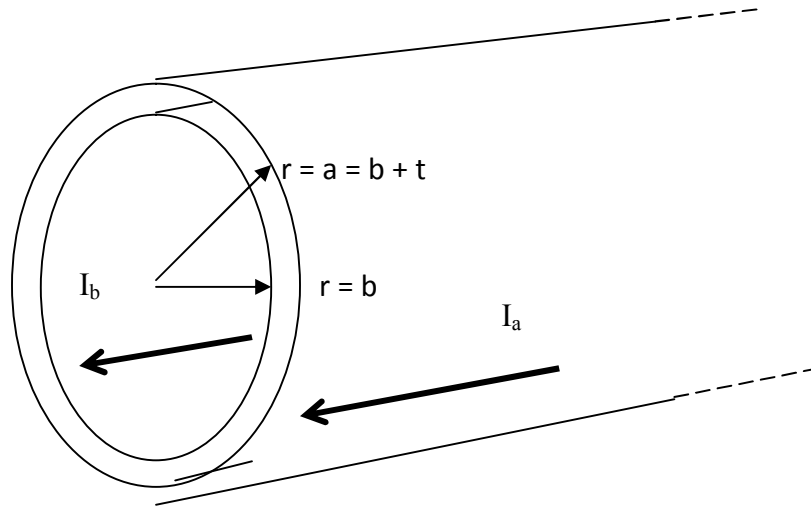


Figure 7. Cylindrical Coaxial Shield

Schelkunoff's coupled shield impedance equations are as follows:

$$(13) \quad \mathbf{E}_a = \mathbf{I}_a \cdot \mathbf{Z}'_a + \mathbf{I}_b \cdot \mathbf{Z}'_{ba} \text{ and}$$

$$(14) \quad \mathbf{E}_b = \mathbf{I}_a \cdot \mathbf{Z}'_{ab} + \mathbf{I}_b \cdot \mathbf{Z}'_b, \text{ where}$$

$I_a$  is the current on the outer surface,  $r = a$ ;

$I_b$  is the current on the inner surface,  $r = b$ ;

$Z'_a$  is the surface or internal impedance per meter of the exterior surface of radius  $a$ ;

$Z'_b$  is the surface or internal impedance per meter of the interior surface of radius  $b$ ; and,

$Z'_{ab} = Z'_{ba}$  is the transfer impedance,  $Z_T$ , per meter between the two surfaces, that is the electric field induced on one surface due to a current on the other.

From 13 & 14, when there is no internal source current,  $I_b = 0$ , and the frequency is so low that the surface impedance equals the transfer impedance,  $Z_a = Z_{ab}$ , the induced electric field along the inner surface is the same as the induced electric field on the outer surface,  $E_a = E_b$ , the first contention of this essay with the same conclusion regarding the induced end-to-end voltages,  $V = \int_0^l \mathbf{E} \cdot d\mathbf{z}$ .

From Schelkunoff's<sup>1</sup> solution to the boundary value problem, with some notation changes reflecting modern usage<sup>2</sup>, these impedances for a length,  $l$ , are as follows including small argument approximations (good to very low frequencies)<sup>1, 2</sup>:

$$(15) \quad Z_b = \frac{\eta \cdot l}{2 \cdot \pi \cdot b} \cdot \frac{[J_0(k \cdot b) \cdot N_1(k \cdot a) + J_1(k \cdot a) \cdot N_0(k \cdot b)]}{D}, \text{ inner surface impedance, where } D \text{ is}$$

$$(16) \quad D = J_1(k \cdot b) \cdot N_1(k \cdot a) - J_1(k \cdot a) \cdot N_1(k \cdot b), \text{ where}$$

$J_n$  and  $N_n$  are Bessel functions of first and second kind, order  $n$ , respectively,

$$(17) \quad a = b + t, \text{ where the braid thickness, } t \ll b < a, \text{ and}$$

$$(18) \quad k \cong \sqrt{i\omega \cdot \mu \cdot \sigma} = (1 + i)/\delta, \text{ the wave factor within the conductor.}$$

The small argument approximation to the internal or surface impedance is

$$(17) \quad Z_b \cong \frac{l}{2 \cdot \pi \cdot b \cdot t \cdot \sigma} \cdot \frac{\sqrt{i\omega \cdot \tau_d}}{\tanh \sqrt{i\omega \cdot \tau_d}}, \text{ where}$$

$$(18) \quad \tau_d = \mu \cdot \sigma \cdot t^2, \text{ the diffusion constant through the conductor thickness, } t.$$

Breaking the internal impedance down further to low and high frequency approximation:

Low frequency,  $\omega \cdot \tau_d < 1$ ,

$$(19) \quad Z_b(\omega \cdot \tau_d < 1) \cong R_{dc} + i\omega \cdot L_{dc}, \text{ where}$$

$$(20) \quad R_{dc} = l / (2 \cdot \pi \cdot b \cdot t \cdot \sigma) \text{ and}$$

$$(21) \quad L_{dc} = \frac{\mu_0 \cdot l}{4 \cdot \pi} \cdot \frac{t}{b}, \text{ the low frequency internal inductance of a cylindrical shell.}$$

High frequency,  $\omega \cdot \tau_d > 1$ ,

$$(22) \quad Z_b(\omega \cdot \tau_d > 1) \cong R_{ac} + i\omega \cdot L_{ac}, \text{ where}$$

$$(23) \quad R_{ac} = l / (2 \cdot \pi \cdot b \cdot \delta \cdot \sigma), \text{ and}$$

$$(24) \quad L_{ac} = \frac{\mu_0 \cdot l}{4 \cdot \pi} \cdot \frac{\delta}{b}, \text{ the high frequency internal inductance of a cylinder or a cylindrical shell, where}$$

$$(25) \quad \delta = \sqrt{1 / \pi \cdot f \cdot \sigma \cdot \mu}, \text{ the skin depth of the material.}$$

The same formulas and approximations apply to  $Z_a$  by replacing “ $a$ ” with “ $b$ ”.

Lightning models will use the low frequency approximation although mumetal shields have small skin depths.

The surface or internal impedance (17) is illustrated in Figure 8 for the real, imaginary, absolute magnitude, and phase of a 36AWG (American Wire Gauge) wire braid shield.

The transfer impedance is given as follows:

$$(26) \quad Z_{ab} = \frac{k \cdot l}{2 \cdot \pi \cdot a \cdot \sigma} \cdot \frac{J_1(k \cdot b) \cdot N_0(k \cdot a) + J_0(k \cdot b) \cdot N_1(k \cdot a)}{D}$$

The small argument approximation for the transfer impedance is as follows:

$$(27) \quad Z_{ab} \cong \frac{l}{2 \cdot \pi \cdot b \cdot t \cdot \sigma} \cdot \frac{\sqrt{i \omega \cdot \tau_d}}{\sinh \sqrt{i \omega \cdot \tau_d}} \cong \frac{e^{-(1+i) \cdot 2t/\delta}}{2 \cdot \pi \cdot \sqrt{a \cdot b} \cdot t \cdot \sigma} \cong R_{dc} \cdot e^{-2t/\delta} \cdot (\cos(\sqrt{\omega \cdot \tau_d}) - i \sin(\sqrt{\omega \cdot \tau_d}))$$

Schelkunoff discusses the sinusoidal behavior in some detail.<sup>1</sup>

■

### Internal Impedance, 36AWG Braid Shield

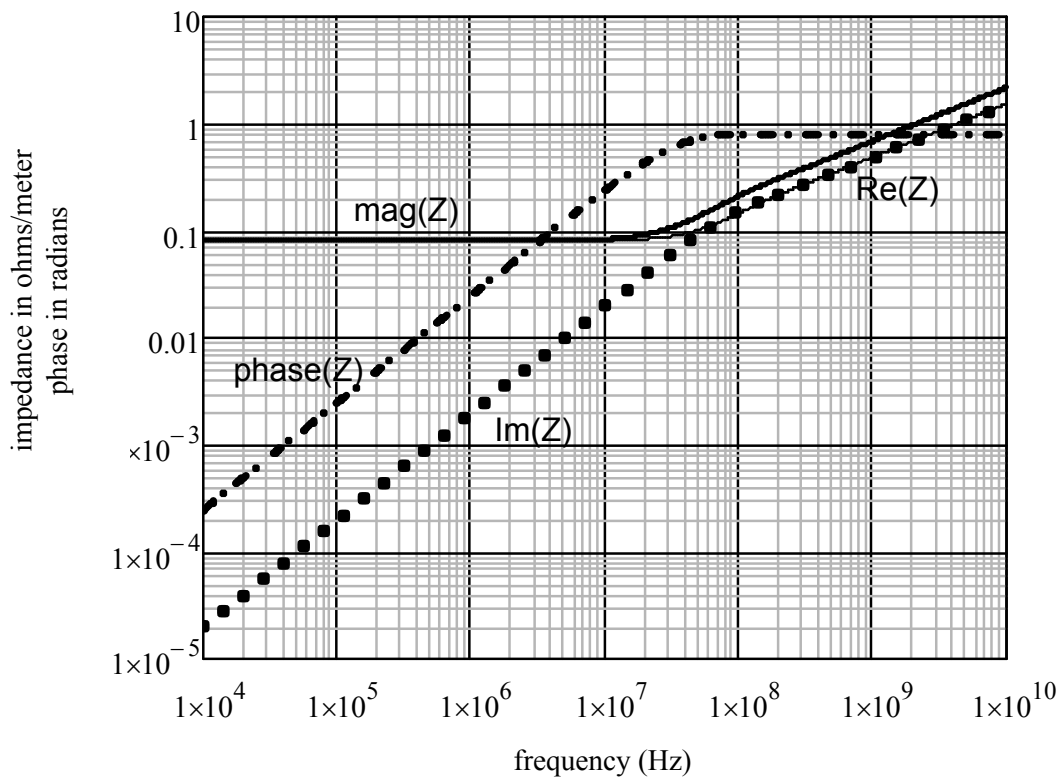


**Figure 8. Internal Impedance Parameters of a 10m Long 1" Radius 36AWG Wire Braid Shield**

The transfer impedance (27) is illustrated in Figure 9 with the phase divided by fifty in order to keep it on the graph.

## Transfer Impedance, 36AWG Wire Braid Shield

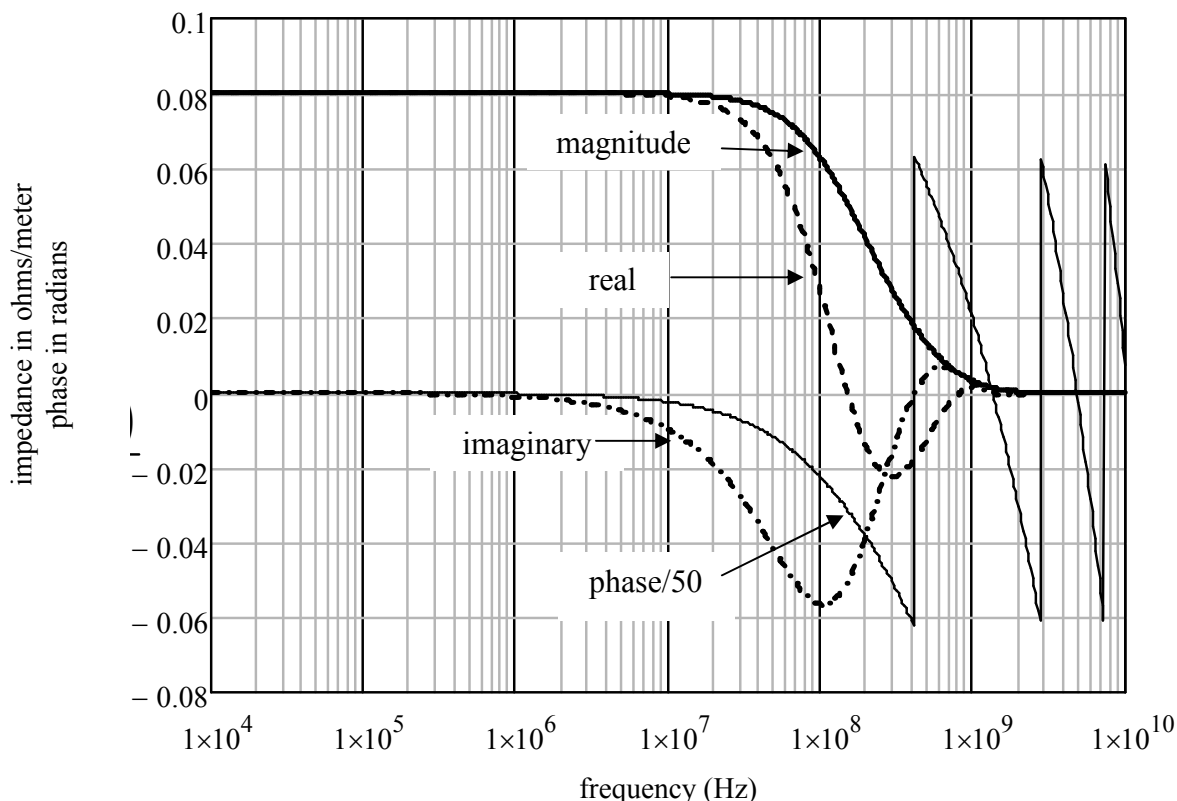


**Figure 9. Transfer Impedance Parameters of a 36AWG Wire Braid Shield**

The surface impedance is approximated as a DC resistance plus an AC resistance proportional to  $\sqrt{f}$  due to the skin depth effect. The transfer impedance is approximated as a DC resistance times an exponential decay through the coax wall according to the  $\sqrt{f}$  skin depth effect, also. When the skin depth exceeds the coax shield thickness, the surface impedances and the transfer impedances become the same, the resistance of the coax shield. The two are plotted below in Figure 10 for a copper 40AWG wire braid shield, showing that the transfer impedance diverges from the surface impedances when  $\omega \geq \tau_d$ . For Waveforms 4 and 5A induced lightning current on the braid, the induced voltage in the shield is therefore about the same inside and out. See Section 4.) Furthermore, the IR-drop voltage across the composite skin controls that across the braid. That IR-drop manifests as a voltage along the braid since the boxes thickness are larger than the skin depth. In order to obtain any shielding effectiveness from a braid shield to such an environment, the wire braid would have to be larger than 20AWG, impractical for widespread use in aerospace vehicles. The solution is the addition of a high- $\mu$  foil to be discussed below in Sections 6 and 7.

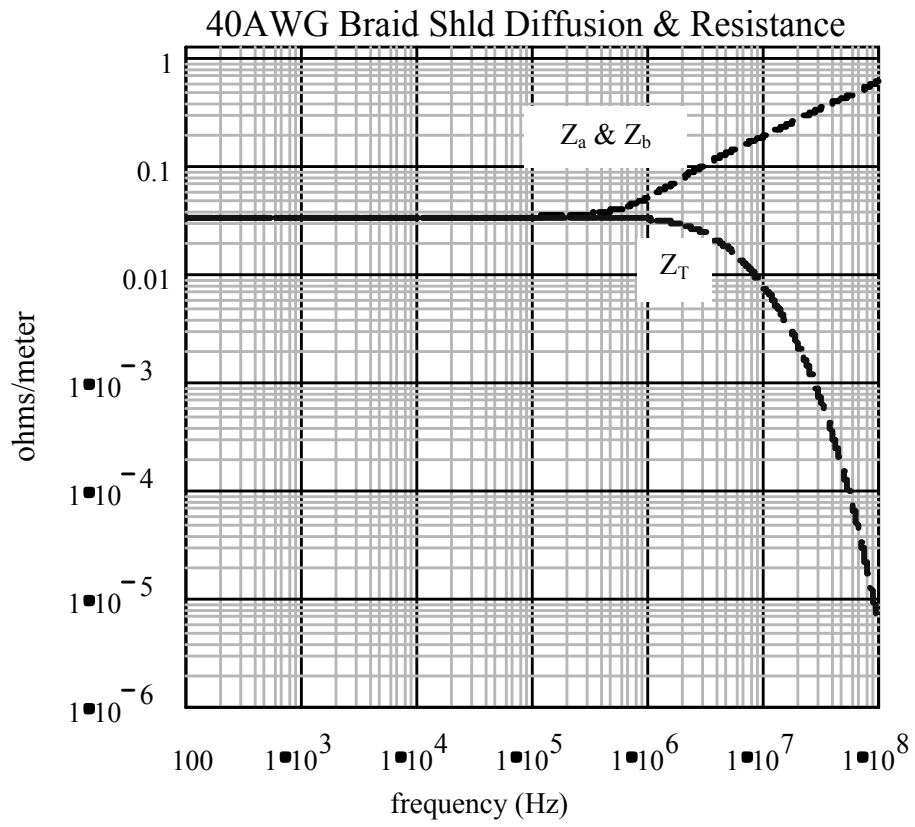


**Figure 10. Surface Impedances and Transfer Impedance for a 40AWG Wire Braid Coaxial Shield**

#### 4. SIMPLE CIRCUIT MODELS OF LOW FREQUENCY CURRENT DIVISION AND CABLE SHIELDING

A low frequency simple circuit model of the combined composite skin and the braid shielded circuit that includes the above diffusion effects is shown in Figure 11, below, for  $\omega \cdot \tau_d \geq 1$ . This is not the usual higher frequency transfer impedance. When  $\omega \cdot \tau_d < 1$ , the internal, external, and shield transfer impedances merge into one parallel impedance,  $Z_a = Z_b = Z_T$ , connected to structure at both ends, shown in Figure 12. Note that  $\omega \cdot \tau_d = 2 \cdot t^2 / \delta^2$ .

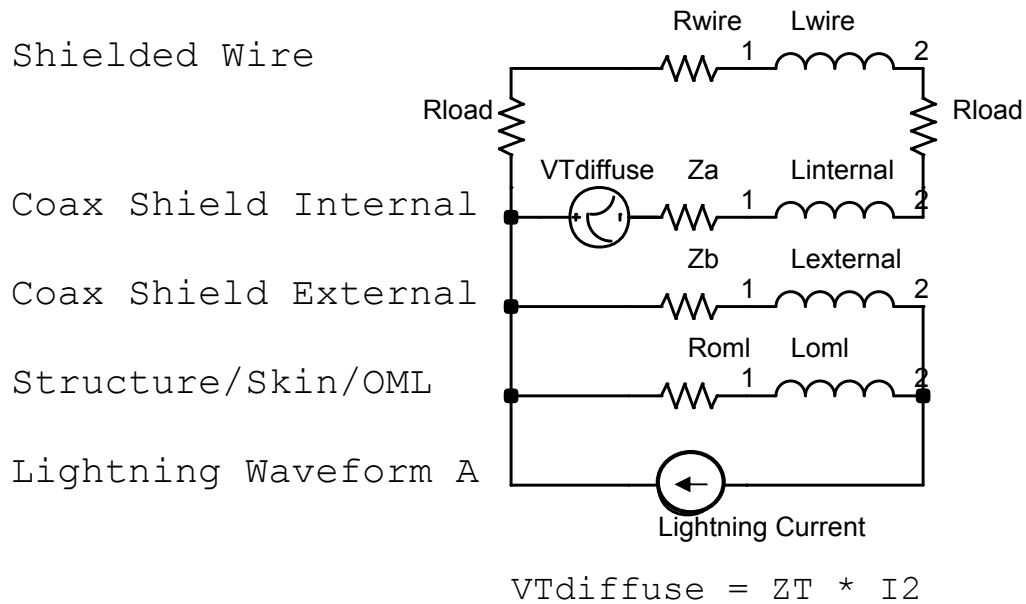


**Figure 11. Simple Low Frequency IR-Drop Circuit Model for Coax Shielding when  $\omega \cdot \tau_d \geq 1$**

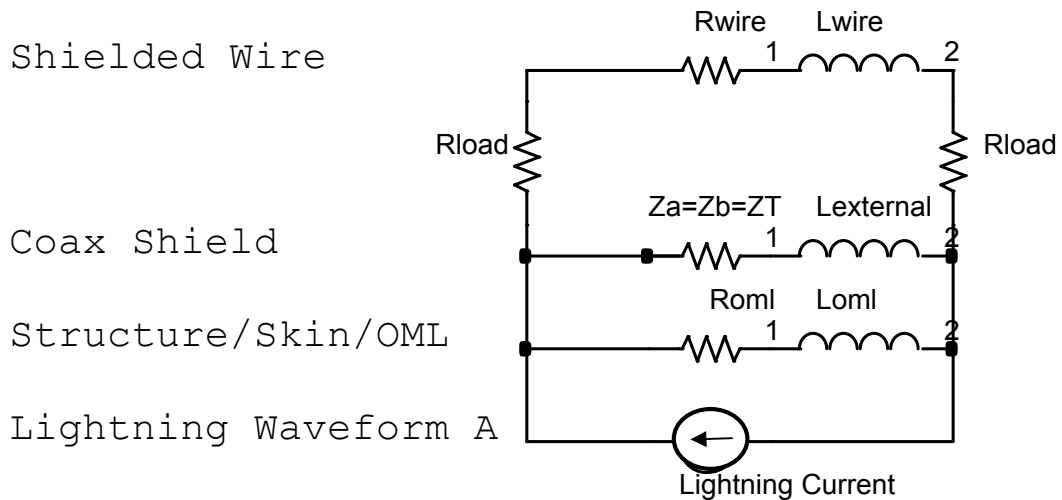


**Figure 12. Simple Low Frequency IR-Drop Circuit Model for Coax Shielding when  $\omega \cdot \tau_d < 1$   
The Most Common Situation in Composite Airframes with WF5A/WF4 on the Copper Braid(s)**

Justification for the model in Figures 2 and 10 is that the current distribution through the braid becomes uniform when  $\omega \cdot \tau_d \leq 1$  thereby making the induced longitudinal electric field,  $E_z$ , and the induced voltage,  $V$ , the same, inside and out. The current distribution is shown in Figure 11, below, for  $\omega \cdot \tau_d = 10^2, 10, 1, 10^{-1},$  and  $10^{-2}$ . This shows that the current is almost uniform through the braid by the time  $\omega \cdot \tau_d = 1$ .

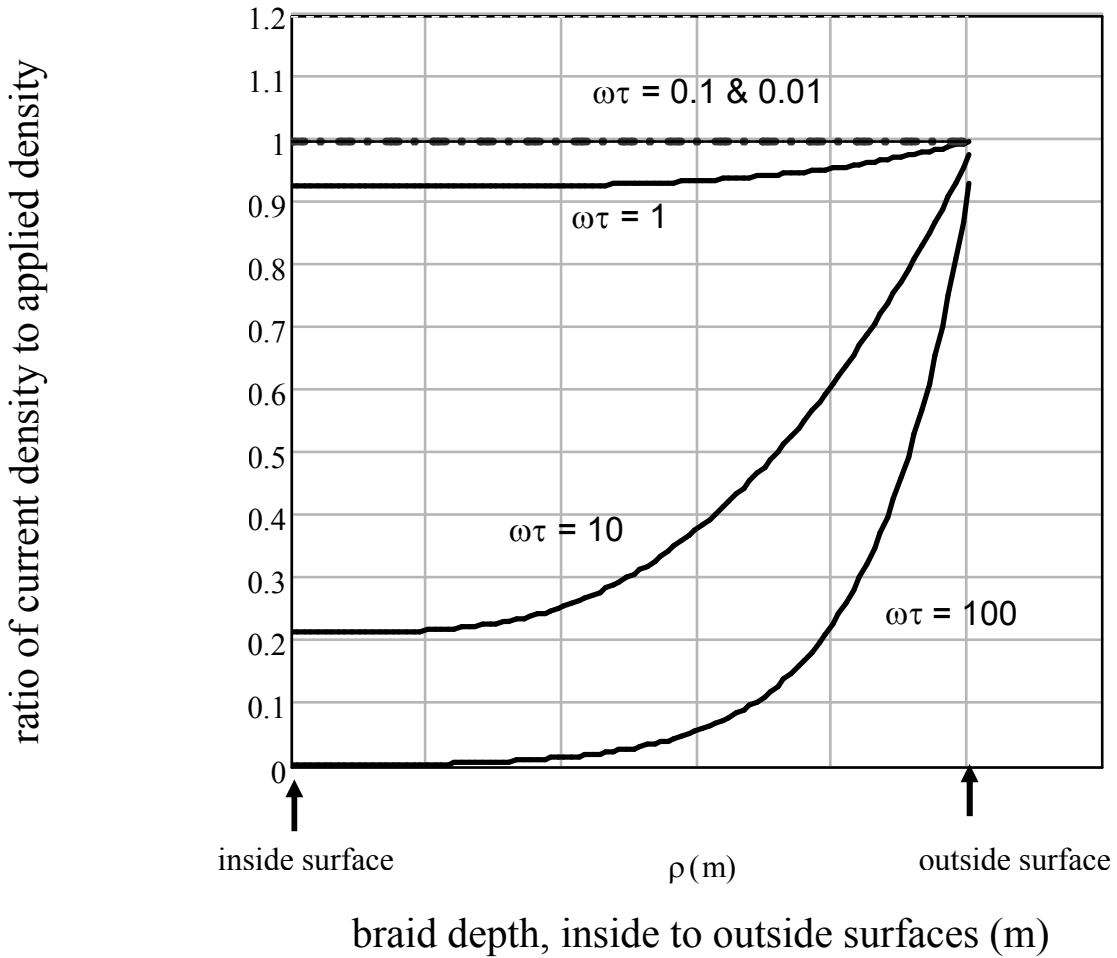


**Figure 13. Current Distribution through Copper Braid/Foil for Different Frequencies Relative to the Diffusion Time,  $\tau$ , when a Current is Impressed on the Outer Surface**

In-flight, the induced voltage and the current division is controlled more by the resistance of the aircraft skin and the cables than by the inductance as in the ground-test configuration.

The voltage induced across a 100m $\Omega$  CFC skin is 13kV, across the same size titanium skin is 33V, and across the same size aluminum skin, 3.2V. The electromagnetic problems associated with CFC airframes is therefore obvious, 72dB worth of problems to solve.

## 5. SUMMARY OF SIMPLE MODELING

The heuristic model in Figure 2 and the circuit models in Figures 11 and 12 provide accurate numbers for the induced open circuit voltage and short circuit current in a shielded wire or an unshielded wire, e.g. the induced voltage will be that developed across the parallel circuit of conductors and the composite airframe, dominated by the composite airframe. The braid shield acts as another impedance across the structure, lowering the induced voltage at the shielded wire loads only a small amount.

This method of modeling and analysis in this paper is recommended as a supplement to and/or correction of SAE ARP5415A, Appendix B.1.1,<sup>5</sup> and the associated text and circuit models with regard to the composite IR-drop induced voltages and currents in shielded and unshielded wires in composite airframes. The individual parameters must be determined for each system. This modeling technique has been criticized because of its simplicity, however it agrees with test data. This paper is intended to provide a theoretical basis for the simple model in the frequency range we are dealing with.

A new cable shield design is presented, below, for shielding the low frequency WF4 induced lightning currents on cable shields, the actual configuration and shield grounding a first in this field.

A new system level ground-test is also under development that eliminates or minimizes the return currents responsible for WF5A cable currents.<sup>25,26</sup>

## 6. COPPER BRAID AND MUMETAL FOIL CABLE SHIELDING

A solution for this problem is high- $\mu$  foil under the copper braid that has a skin depth small enough to actually shield the low frequency Waveform 4 currents. The high- $\mu$  foil must be overlapped by, say, 20-30% to maintain contact, maximize optical coverage, and keep the magnetic reluctance low.

The possible drawback is saturation from high currents of the high- $\mu$  material rendering it ineffective, also. A comparison of the transfer impedance of a foil of the same thickness is shown below in Figure 17. The nickel doesn't have high enough permeability to improve the attenuation down to Waveform 4 frequencies. The mu-metal with  $\mu_r \geq 10,000$  lowers the diffusion curve below the 10-25 kHz frequencies in order to attenuate Waveform 4. The high frequency transfer inductance is not shown in order to highlight the low frequency diffusion. The high- $\mu$  metals are ferrous-nickel alloys therefore their conductivity is at least 3-5 times lower than copper.

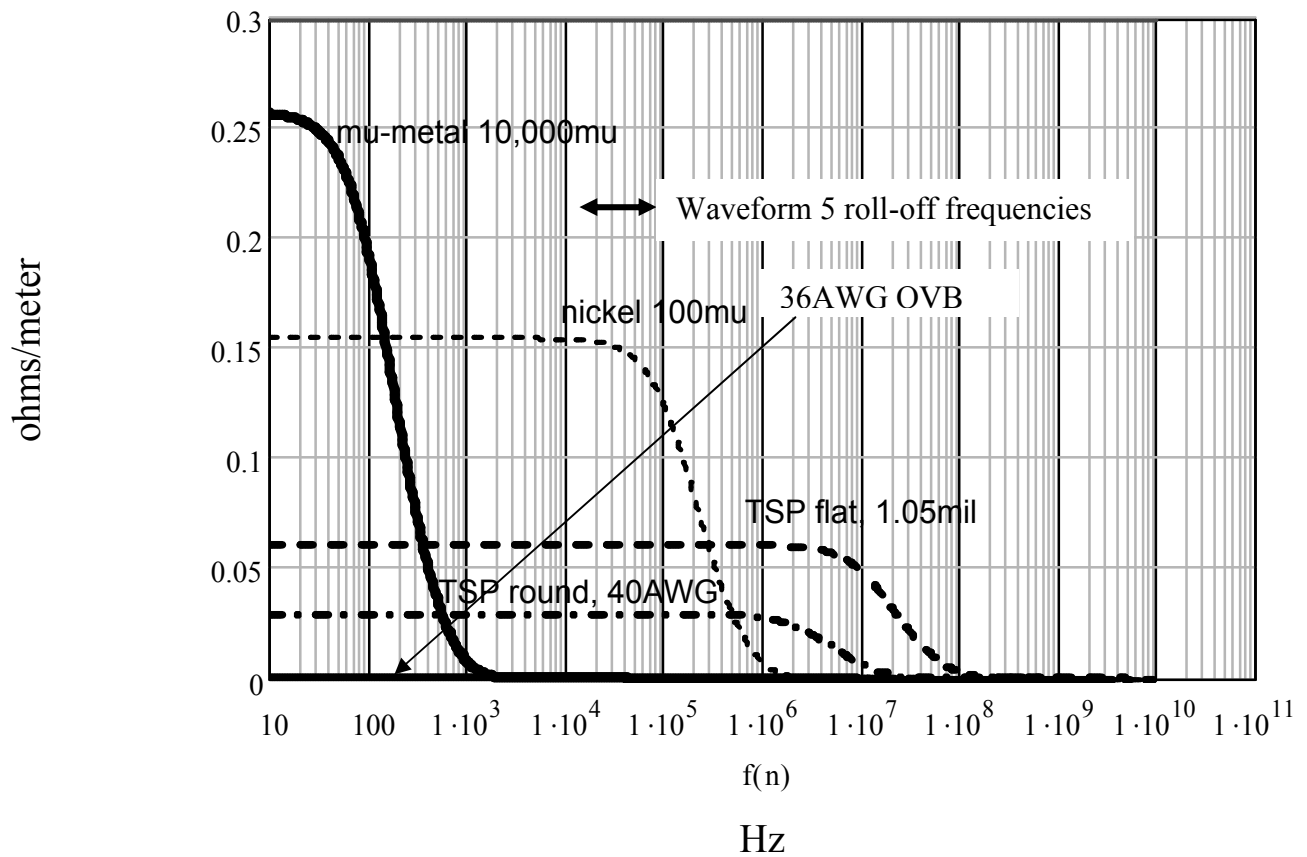


**Figure 14. Copper Braid versus High-Mu Foil for Low Frequency Shielding**

Raychem makes a “superscreen” with one and two high-mu foil layers and have published the following shielding data, Figure 20, showing the dramatic improvement in low frequency shielding<sup>9</sup>. With another layer of braid and foil, Raychem shows another 60dB improved shielding, 10-25kHz. Actually, this data is fictitious because the inner copper braid will shunt current past the mumetal foil rendering it useless. Test data on the superscreen reveals that it, indeed, shields like a double copper wire braid shield with high optical coverage and no mumetal.<sup>11</sup>

A new layered copper and mumetal cable shield<sup>22</sup> has been designed and built per the original IN608 and is described below in Section 7.

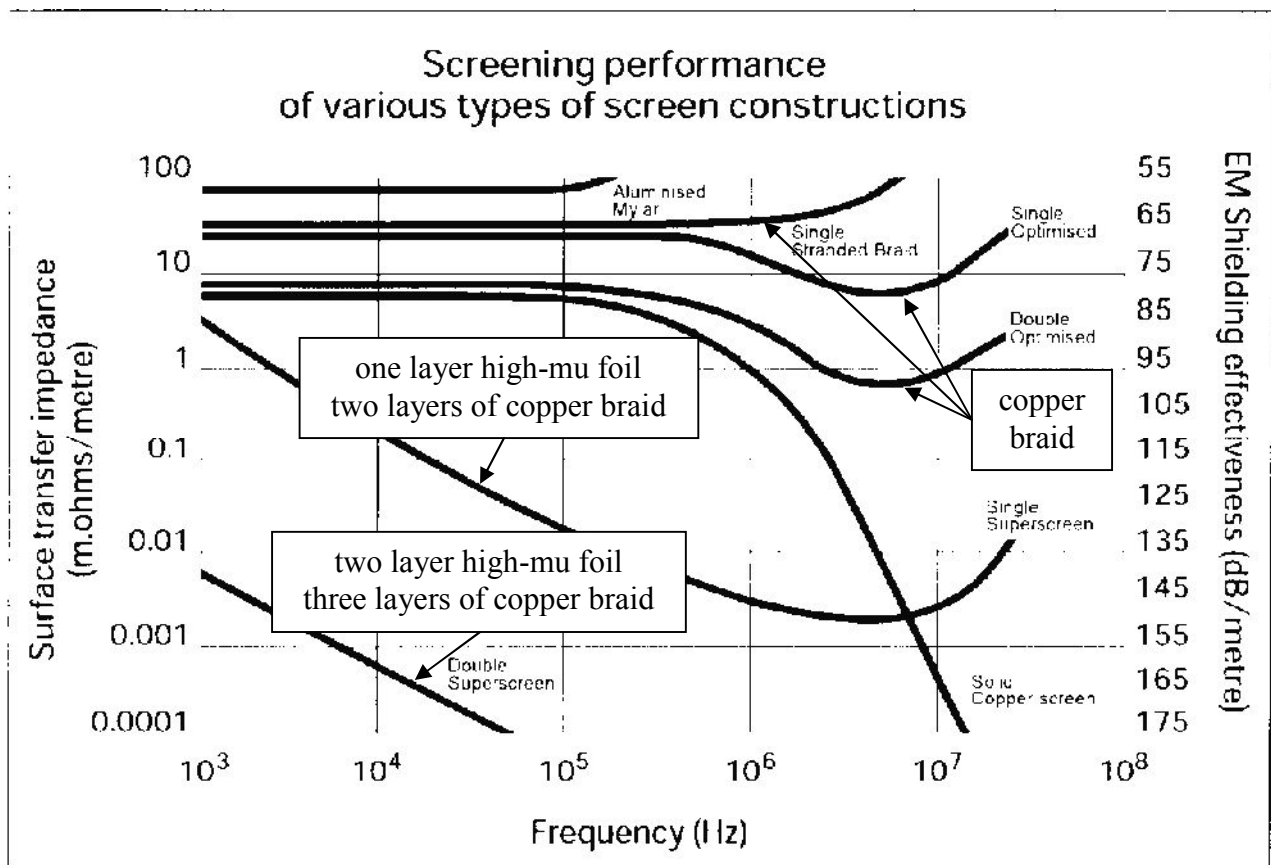


Figure 15. Raychem Advertized “Superscreen” with High-Mu Foil Compared to Copper Braid<sup>9</sup>  
 (See Figure 19 for superscreen cables with high-mu foil.)

D. E. Merewether modeled the saturation effects of ferromagnetic materials used in coax shields<sup>7,8</sup>. A notional graph of such effects is in Figure 16, B versus  $\mu(H) \cdot H$ , showing the sharp drop in relative permeability above the saturation field level,  $B_s$ . That renders the foil much less of a shield above some level of induced current/field. A real saturation graph with data is in Figure 17 where  $B_s$  is fuzzier.<sup>10</sup>

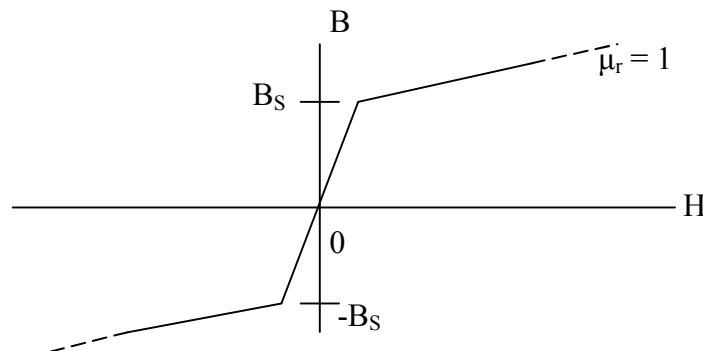
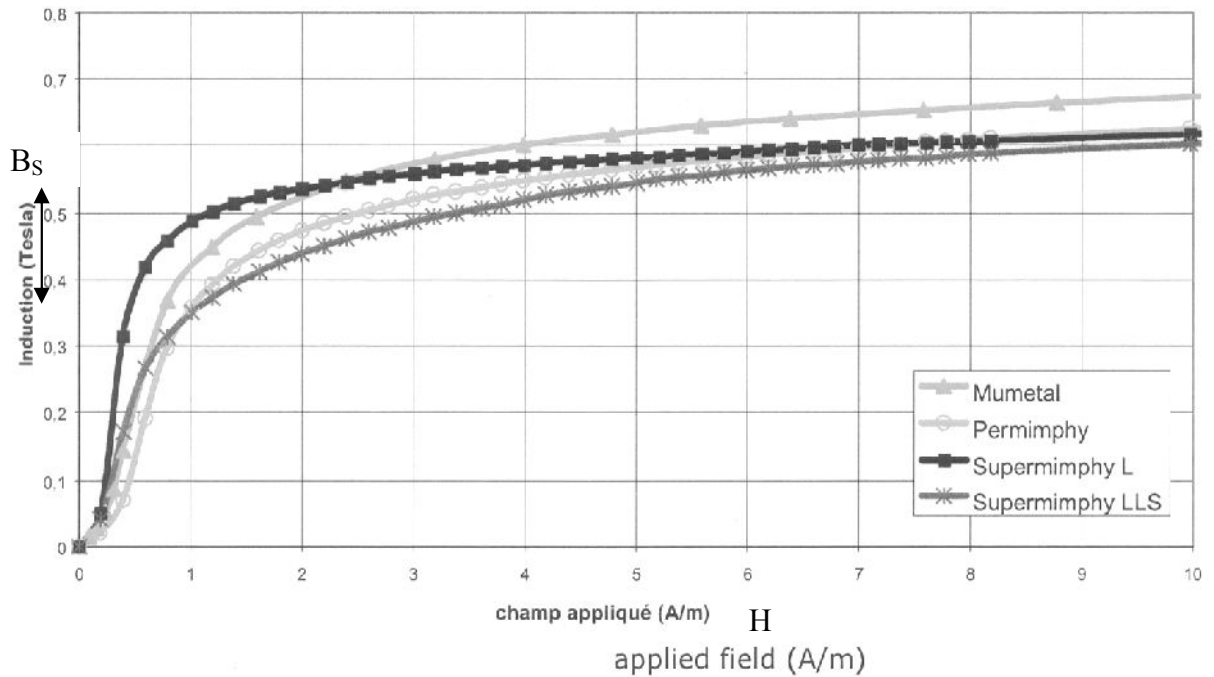


Figure 16. Notional Graph of Ferromagnetic Saturation Effect

As the field increases and the mu-metal saturates, its permeability eventually decreases to that of free space, i.e.  $\mu_r \rightarrow 1$ .<sup>2</sup>



DC magnetization curves for Mumetal, Permimphy, Supermimphy L and Supermimphy LLS.

**Figure 17. Typical High-Mu Metal Magnetization Curves from ArcelorMittal<sup>10</sup>**

Merewether developed a simple prescription to see how thick of a foil was needed before it was saturated all the way through using a damped sinusoid.<sup>7,8</sup>

$$(28) \quad t_{sat} \approx \frac{1}{\pi} \cdot \sqrt{\frac{I_p}{\sigma \cdot B_s \cdot f \cdot R}}$$

where

$I_p$  is the peak current,

$\sigma$  is the conductivity,

$B_s$  is the material's saturation level,

$f$  is the frequency,

$t_s$  is the foil thickness to prevent total saturation, and

$R$  is the cable shield radius.

Lightning Waveform 4 is not sinusoidal. However, we will use this simple prescription until we derive a better one. Its time-to-peak is 40 $\mu$ s corresponding to a frequency of about 25kHz. Its fall time is about 88 $\mu$ s corresponding to a frequency of 10kHz. Its conductivity is about x5 less than copper or roughly 10<sup>7</sup> mhos/m. The saturation level used here is 1.53W/m<sup>2</sup>, the same as Merewether used. With a peak current of 1kA at 25kHz, all of this gives us a minimum foil thickness of 1mm or 2.54 mils, close to the thickness of a 40AWG wire. More investigation will come up with the best material with the least weight penalty including a copper overbraid to absorb most of the current and perhaps another layer of foil as in the Raychem example. This example is too crude to use for design, meant only to "ballpark" the numbers from Merewether's model, the 2½ mils being a good sign. A copper overbraid will reduce the current in the high-mu foil by about 600, therefore a 1 mil thickness mumetal foil will suffice for this example. The above Raychem foil is 2 mils thick<sup>11</sup>.

The voltage induced within a cable shield is as follows:

$$(29) \quad V(t) = \int ds \cdot e^{s \cdot t} \cdot Z_T(s) \cdot I_{cable}(s)$$

where  $I_{cable}$  is that induced in-flight, equations 6,9 & 10 by a 200kA Component A strike.

The transfer impedance (27) is approximated at low frequencies as follows:<sup>10</sup>

$$(30) \quad Z_T \approx R_{DC} / (1 + s \cdot \tau_d)$$

As an example with copper wire braid shields, the induced lightning voltage from a Component A current in a CFC in-flight airframe with several copper shields of varying thickness is illustrated below in Figure 18. Table 1 contains the AWG versus metric thicknesses and other shield parameters. The induced lightning voltage from a Component A current in a CFC in-flight airframe with a 1 mil foil shield is shown below in Figure 19 for a range of relative magnetic permeability,  $\mu_r$ , from about 100-to-10,000. The copper braid is ineffective and the mumetal is demonstrably superior.

■

### Induced Voltage, Shielded, In Flight

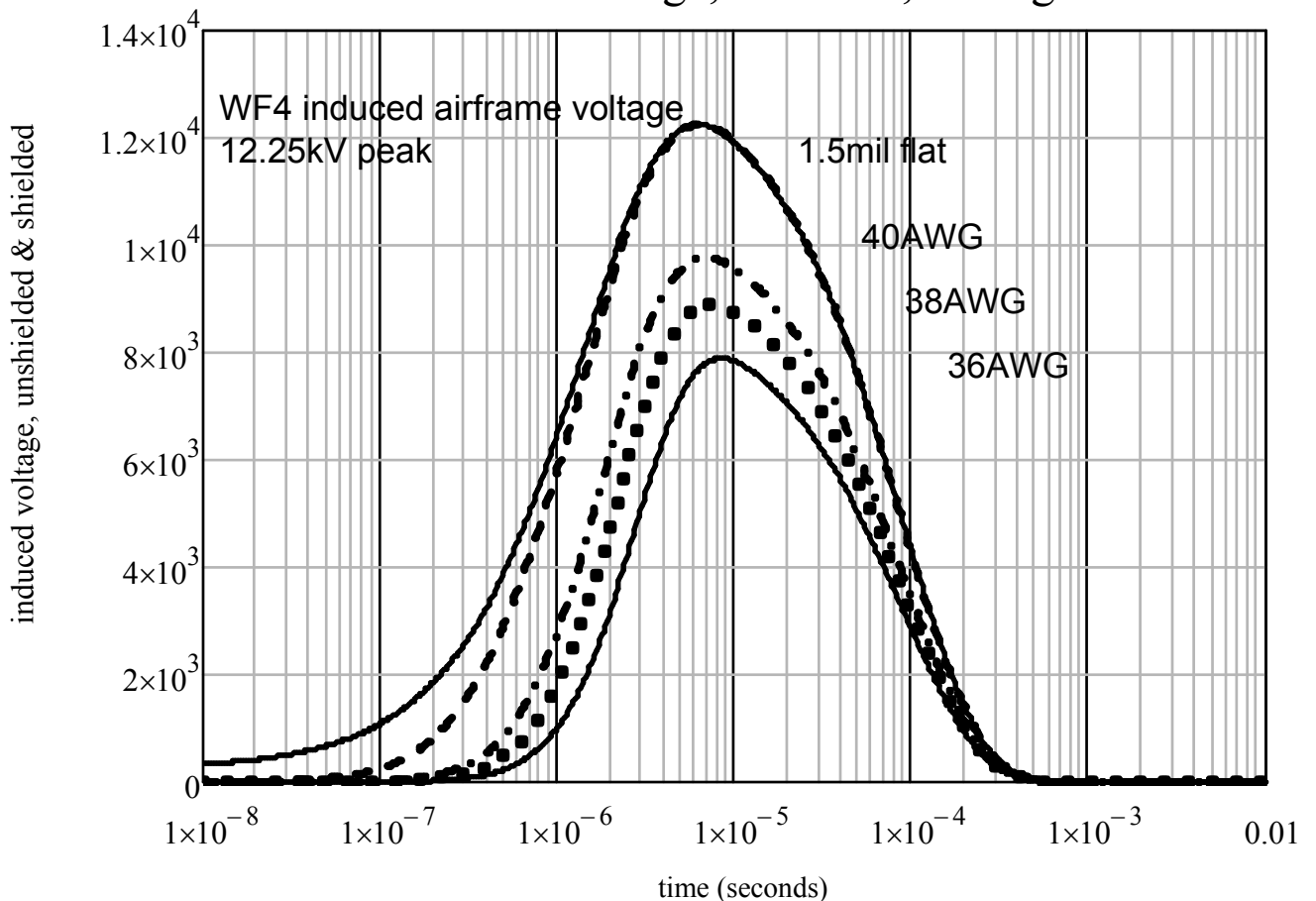
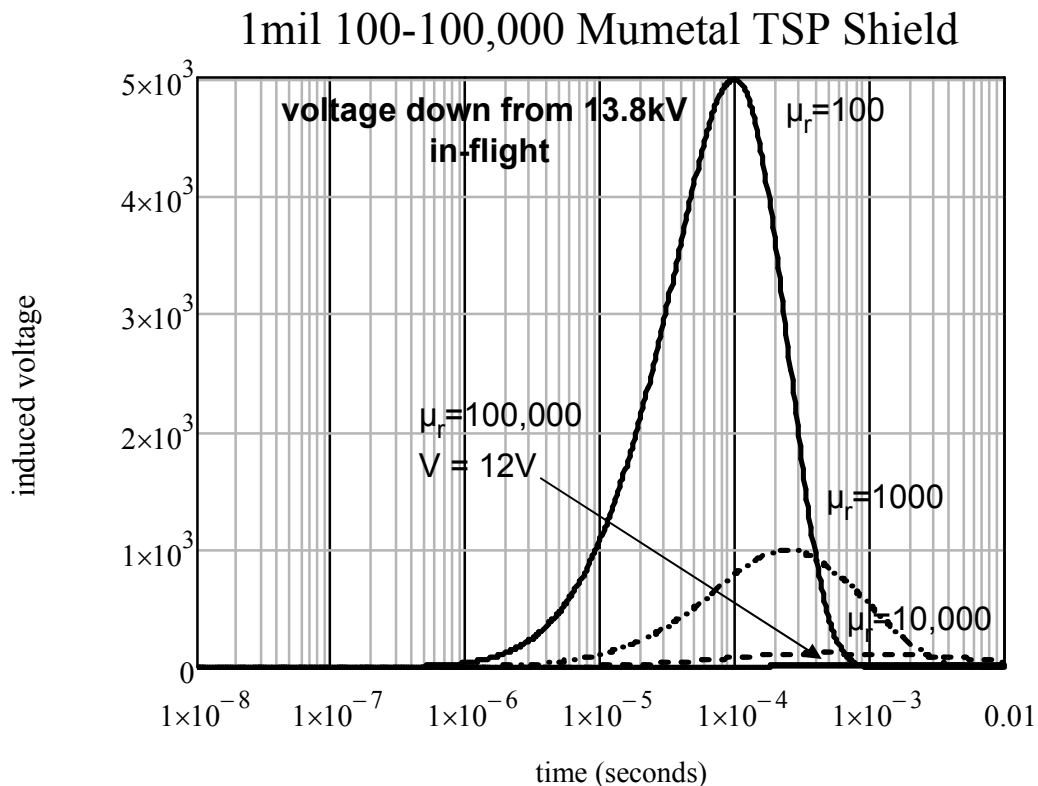


Figure 18. Induced Voltage In-Flight with different Thicknesses of Copper braid

**Table 1. Cable Shield Parameters**

shield type	braid size	thickness t(m)	diam. (inches)	diffusion time, $\tau_d$	DC $R_{dc}$ ( $\Omega/m$ )	f at $R_{dc}=R_{ac}$
copper foil braid	1.5 mil	$3.8 \cdot 10^{-5}$	¼"	105ns	36m $\Omega/m$	3MHz
copper wire braid	40AWG	$8 \cdot 10^{-5}$	¼"	467ns	17m $\Omega/m$	682kHz
	38AWG	$10^{-4}$	1"	729ns	2.2m $\Omega/m$	437kHz
	36AWG	$1.27 \cdot 10^{-4}$	1"	1.18 $\mu$ s	1.7m $\Omega/m$	318kHz
	34AWG	$1.6 \cdot 10^{-4}$	1"	1.87 $\mu$ s	1.4m $\Omega/m$	170kHz

■



**Figure 19. Induced Voltage In-Flight with Varying Permeability 1 mil Cable Shield**  
**Add Copper Braid and Reduce by 1/600 or 56dB**  
**5m Connectors add 100V**  
**Saturation Ignored**

We need to add a layer of copper braid on top of this in order to reduce the current on the high-mu foil by about 600 and the induced voltage by the same. The layered shield problem is not trivial<sup>1</sup> although we can scale it simplistically.

The trade off then includes the following parameters: (1) one or more layers of copper braid and/or foil, (2) foil permeability, (3) foil saturation level, (5) foil conductivity, and (6) foil thickness. The Raychem superscreen cable was allegedly developed for lightning protection on a very big Boeing airplane.<sup>11</sup>

The superscreen cable has a flaw; that is, the inner copper braid in Figure 20 will conduct current around the high- $\mu$  foil, thereby negating the shielding by the foil. Test results then show low frequency shielding more like a 30AWG copper braid than a high- $\mu$  foil.<sup>11</sup> Installing any copper shield underneath the high- $\mu$  foil will do the same thing. The solution is to isolate the inner braid from the high- $\mu$  foil and ground the inner copper braid at one end only as Raychem has done per the information in this paper.<sup>22</sup>

The double superscreen in Figure 20 is the same mistake repeated twice.

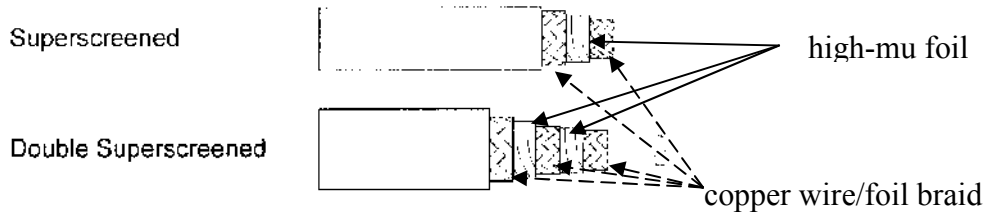


**Figure 20. Raychem Superscreen Shielded Cables<sup>9</sup>**

We need the copper braid or foil next to the wires because the high- $\mu$  foil is too lossy due to (1) the DC resistance and (2) the reduced skin depth. The two surface impedances are shown in Figure 21 where the impedance of the high- $\mu$  foil is about x600 (58dB) higher than the copper braid above a certain frequency.

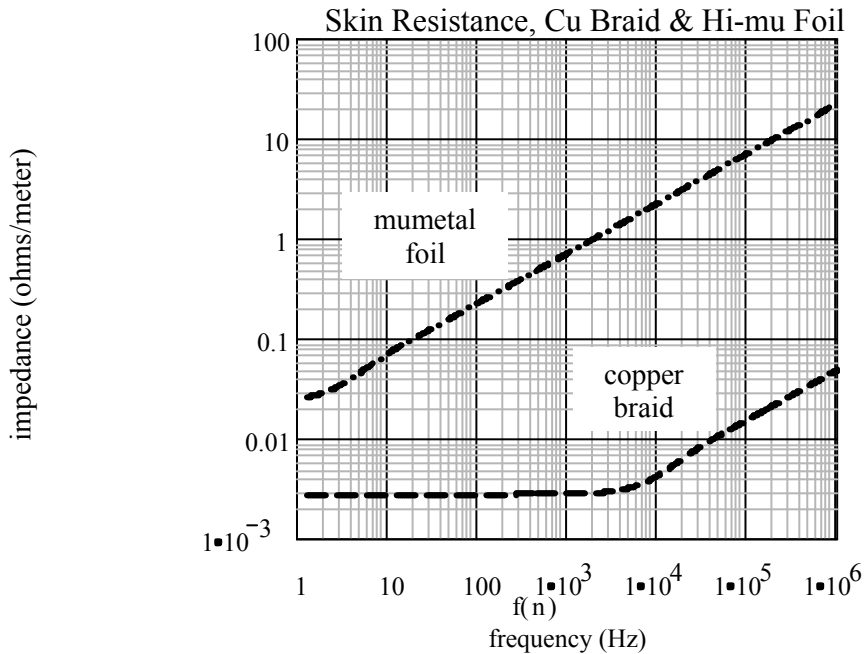


**Figure 21. Impedance of Copper Braid and High- $\mu$  Foil**

This large difference in impedance will enhance the apparent shielding effectiveness more than with either the copper or foil by themselves, i.e. it will be this ratio times the transfer inductance of the mumetal foil.

## 7. NEW LAYERED COPPER BRAID & HIGH-MU FOIL WITH INNER COPPER LAYER

Appendix A is a draft spec control drawing (SCD) of the new cable. Appendix B is a transfer function measurement on the cable with the method in MIL-C-85485, both courtesy of R. Moore of Tyco/Raychem.<sup>11</sup> The DC resistance is higher than expected from a single layer 38AWG copper wire braid, a phenomenon Mr. Moore informs us is common to all of the layered copper braid over a mumetal foil. This author takes issue with the test method because (1) the cable is too short (2) it's terminated in a short and resonates, and (3) it adds a portion of erroneous data proportional to  $\sqrt{f}$  above 10MHz that is not in any theory or any other test method. The non-ferrous connectors are obviously controlling the entire range of data, as expected, although the DC resistance is high and the diffusion roll off frequency is high.

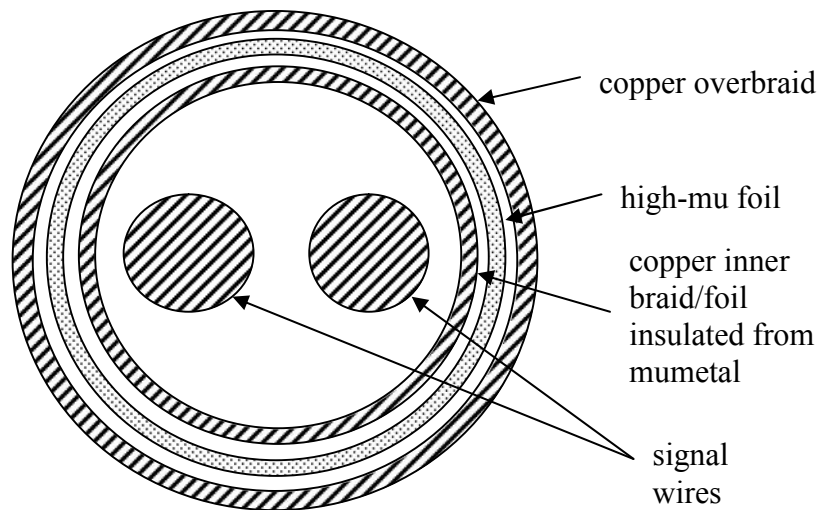


**Figure 22. WF5A/4 Cable Design: Copper Overbraid, High-mu Foil, & Copper Inner Braid/Foil Insulation in between all the Inner Copper Braid and the Mumetal Foil<sup>22</sup>**

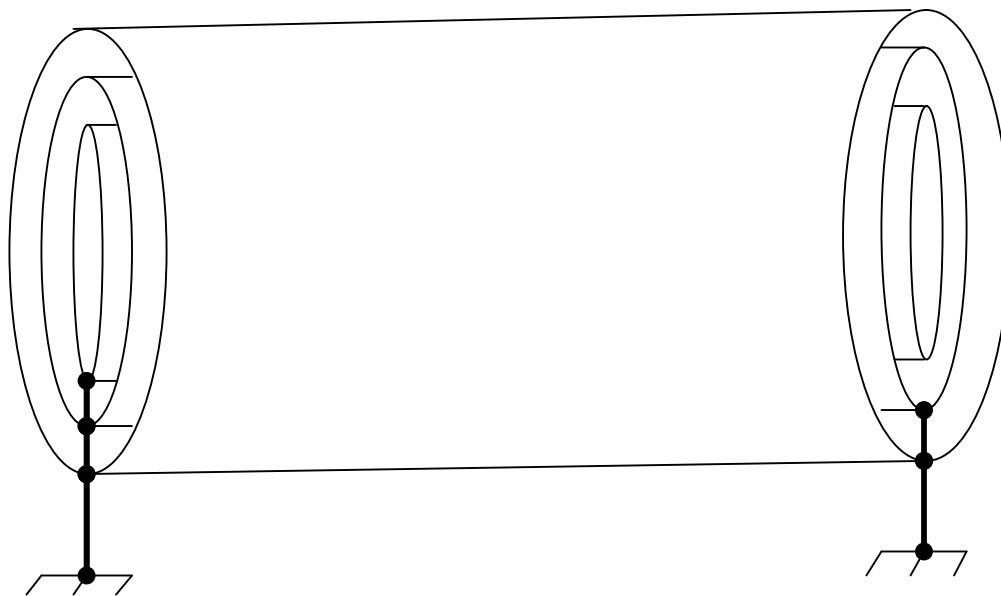


**Figure 23. Grounding Scheme for the Lightning Cable Shield Design Inner Copper Layer grounded at One End Only<sup>22</sup>**

Figure 24 is the system circuit model including the layered copper braid and high-mu foil. The innermost braid has been left out since we will ground it at one end only, effectively removing it from this shield diffusion model.

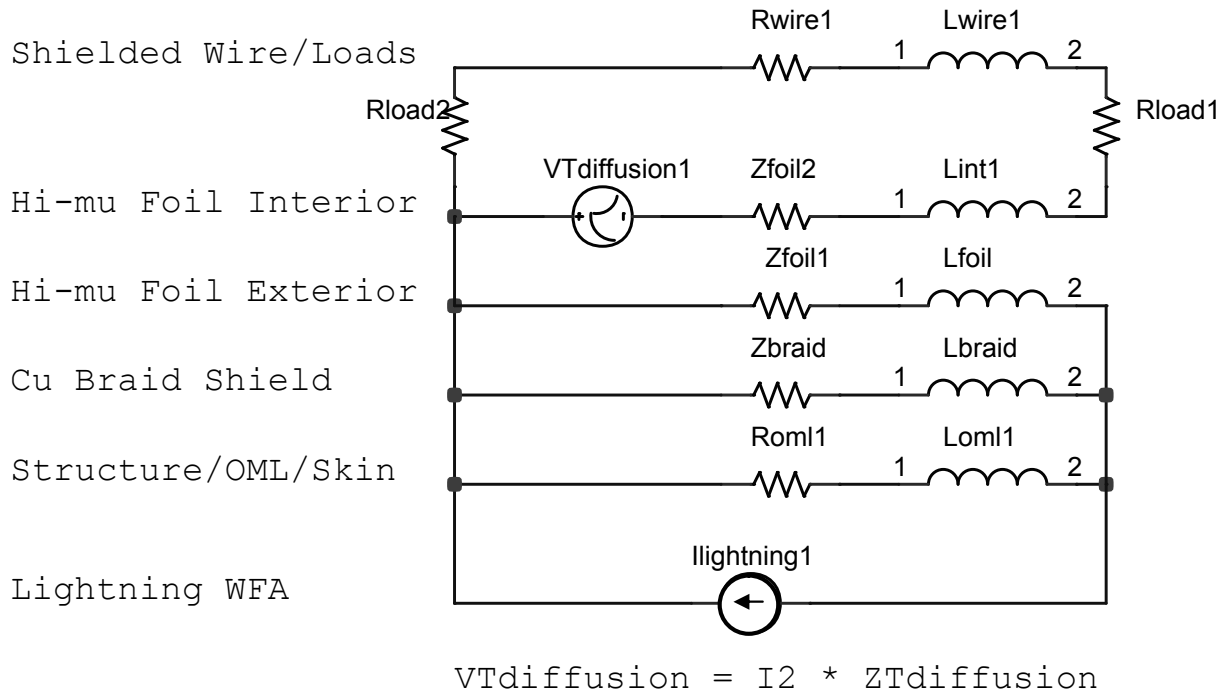


**Figure 24. System Circuit Model with Cu Braid & High-mu Foil Wire Shield**  
**Assumes  $\omega \cdot \tau_d \leq 1$  in the Copper Braid,  $\omega \cdot \tau_d \geq 1$  in the Foil**

The induced voltage,  $V_{Tdiffusion}$ , is the following in the frequency domain, illustrating the enhancement due to the impedance difference between the copper braid and the high-mu foil in Figure 26:

$$(31) \quad V_T = \frac{Z_{braid} \cdot Z_{foil}}{Z_{braid} + Z_{foil}} \cdot I_{cable}$$

where over the frequency range of interest, 10-10<sup>5</sup> Hz, the ratio of impedances which is the ratio of currents is about  $\sqrt{\frac{\sigma_{braid}}{\mu_r(foil) \cdot \sigma_{foil}}} \approx \frac{1}{600}$ . The ratio of currents is shown in Figure 25.

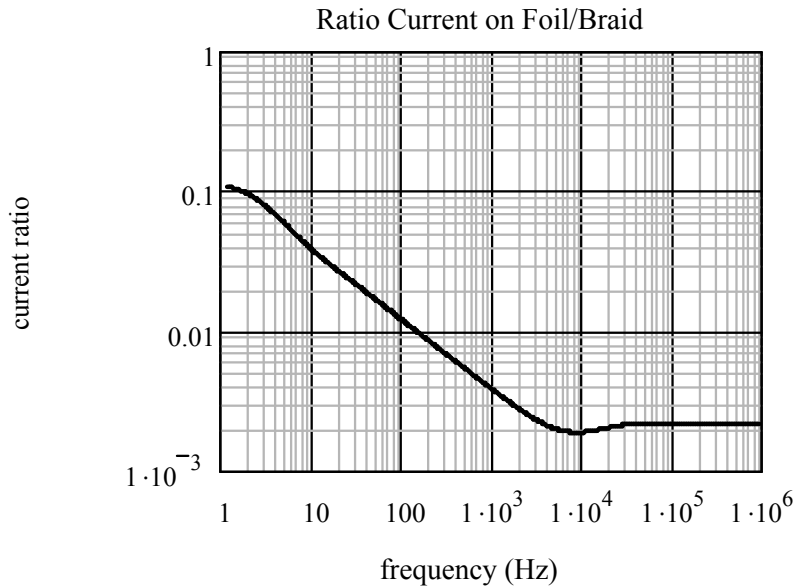


**Figure 25. Ratio of Current on High-mu Foil/Copper Overbraid**

The equivalent transfer impedance of the two layers of shielding is the product of the above two functions. The voltage induced when a current is applied to the layered shield is as follows:

$$(32) \quad \mathbf{V}_T(t) = \int_0^\infty ds \cdot e^{s \cdot t} \cdot \frac{Z_{braid}(s) \cdot Z_{foil}(s)}{Z_{braid}(s) + Z_{foil}(s)} \cdot \mathbf{I}_{cable}(s)$$

The shielding effectiveness of the high-mu foil is considerably enhanced and saturation of the foil is greatly decreased by the copper overbraid due to the resulting reduction of current on the foil.

The transfer impedance of the cable shield alone from peak induced voltage to peak Waveform 4 or 5A current is therefore 10 micro-ohms per meter. That will attenuate the 100kA Waveform 4 current to 1V/m.

The combined cable shield is so good that the overall shielding effectiveness will be controlled by the non-ferrous connectors. A layered boot with high-mu film would be necessary to come close to the cable shield itself. These numbers will increase when 5-10mΩ connectors are included, in fact increase to about 5-10V for a 1kA shield current.

Appendix A is the draft specification control drawing of the new cable.<sup>11</sup>

Appendix B is the transfer impedance measured by Tycoelectronics/Raychem with the method of MIL-C-85485.<sup>11</sup> This author takes issue with this method because (1) the cables is too short rendering the data more representative of the connectors than the cable, (2) the cable is grounded in short circuit instead of in a matched load creating resonances not part of the transfer impedance, and (3) this method always creates the  $\sqrt{f}$  rise in perceived transfer impedance above 1MHz that is not in any theory or any other test data. The DC resistance higher than the copper braid alone is always seen in such cables with a mumetal foil according to Raychem.

## 8. EFFECTS OF THE OPEN SHIELD ON THE DIFFERENTIAL & COMMON MODE SIGNALS

There is a question about the effects of the inner copper layer being open at one end on the signals passing through. If the shield is grounded, the reflection coefficient,  $|\Gamma| = 1$ . If it's floating, the reflection coefficient,  $|\Gamma| = 1$ . Pick your poison. They're both mismatched with respect to common mode.

Presuming twisted shielded pairs or twinaxial shielded wires, the differential currents in the inner shield take a "U-turn"<sup>14</sup> at the discontinuous ungrounded ends, Figure 26, better described as an inductive short circuit with a voltage reflection coefficient of  $\Gamma_V \geq -1$ . Common mode shield currents see a capacitive open circuit, Figure 27, with voltage reflection coefficient of  $\Gamma_V \leq +1$ .

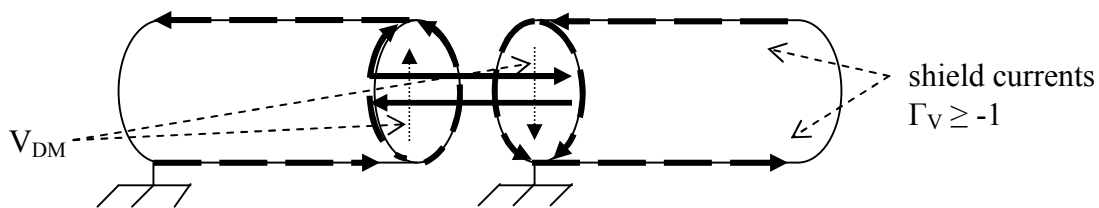


Figure 26. Differential Mode Shield Currents at Shield Gap

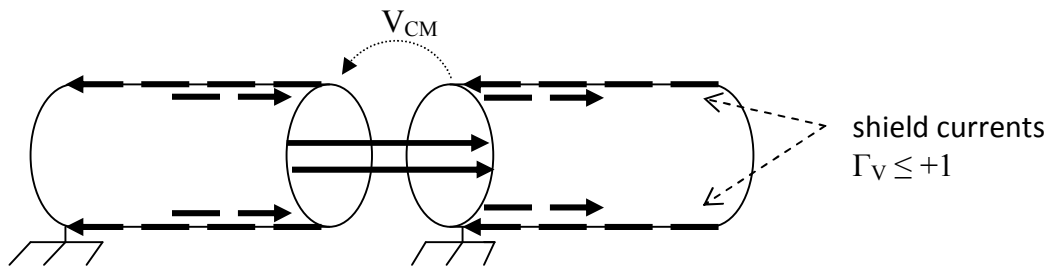


Figure 27. Common Mode Shield Currents at Shield Gap

The differential shield currents making U-turns at the open gap in the shields will induce electric fields across the pair of wires traversing the gap of about equal and opposite polarities on either side. The gap is never more than a few millimeters which is small compared to a quarter wavelength of 7.25 centimeters of, say 1GHz signals, therefore the two oppositely polarized differential mode voltages should be of small consequence.

Common mode currents and voltages in the inner shield layer will reflect off of the open ends resulting in about twice the incident voltage at the gaps in the shield layer. Let's examine two examples, RS422 signals and Ethernet signals.

RS422 line drivers put out as much as 3 volts of common mode<sup>15</sup> which when reflected at the open gap in the inner shield layer will result in 6 volts across the gap assuming one side of the gap grounded and the other side open. RS422 line receivers have a common mode tolerance of  $\pm 7$  volts<sup>16</sup> making the open gap acceptable but with little margin.

Ethernet circuits put out 1.5-2.5 peak-to-peak volts differential mode<sup>16</sup>. Ethernet receivers tolerate about that amount of common mode<sup>17</sup>. Conversion of differential mode to common mode is tightly

controlled in the transmit and receive circuits, the cables, and in the connectors. Taking an Ethernet cat7 connector for example; the mode conversion, called “transverse conversion loss” (TCL) in the IEC Standards<sup>17</sup>, is specified to be no worse than  $TCL(dB) = 66 - 20 \cdot \log(f(\text{MHz}))$  which at 1GHz is 6dB. Reflections of twice the incident voltage or 6dB wipe out the mode conversion (TCL) of the connector making the gap in the inner shield layer a potential problem, particularly with more than one connector in the line so shielded.

Siemon experts say that we could put a single point ground (SPG) shield with a gap on one end of the foil shielded twisted pairs (FTP) shielded cat6 Ethernet cable but not the cat7 because cat6 retained the mode conversion controls in the twisted pairs.<sup>13</sup> Cat7 relaxed this feature because the shielding took care of the crosstalk and EMI immunity with less balance control needed in the wiring. Transformer coupling can further take care of most of the common mode problems on Ethernet and Time Triggered Gigabit Ethernet (TTGbE).

Keep in mind that this shield design is for those cables in a composite airframe exposed to the large Waveform 4 IR-drop voltages with the Waveform 5 currents on the cable shields. For those lines, both the older technology RS422<sup>19</sup> and 485 as well as the newer technology Ethernet<sup>21</sup> and TTBGE, there are now transformer and opto-isolation techniques with 1kV stand-off capability in the transformers. The transformer circuits with bifilar chokes also provide about 30-50dB of common mode isolation, more than enough to handle the 6dB spikes in the common mode voltage induced by the gap in the inner layer of shielding.

The last mitigation process for Ethernet and TTBGE systems is adaptive software whereby the line driver and/or the line receiver detect the errant signals and cancel them out at either or both ends. One or both of the line driver or line receivers are programmed to recognize the change in the signals received due to insertion loss, impedance changes, and reflections and are programmed to negate those signals to an acceptable level of bit error rate.<sup>14</sup> These techniques were developed when designers realized that mode conversion, crosstalk, and EMI are always present with unpredictable levels and effects, therefore the software “encryption” was designed to correct, ignore, or cancel out the errant signals caused by the EMI/EMC effects. The motivation to do so was furthered along by the problem Ethernet designers have with wire and cable shielding in that it is never maintained up to standards and, in fact, presents a safety violation when connected to two terminals operating off of two different power mains.<sup>13</sup>

As an aside, wire and cable shielding is more of a problem for American designers than European designers because American EEs have never come to grips with the “ground-loops” that result from shields grounded at both ends, i.e. they believe that the shield in the noise ground loop is less desirable than the circuit in the noise ground loop. EMI engineers make careers countering this errant motherhood.

## 9. CONCLUSIONS

There are three ways to reduce the lightning induced voltage IR-drop in wiring running over lengths of composite structure:

- (1) The obvious – make those lengths of external skin out of aluminum or titanium, worth 40-60dB;
- (2) Install a low resistance, low inductance, groundplane underneath all wire runs, worth 8-12dB, easy to do in aircraft fuselages, difficult to impossible in wings, empennages, missiles, rockets, etc.; and,
- (2, rev A) The new in-flight model with internal inductance instead of external inductance eliminates the extreme width requirements for low inductance, therefore, it is easier to install a low resistance groundplane in a smaller space.
- (3) Install one or two high- $\mu$  foil layers underneath the copper overbraid to shield the low frequency Waveform 5 current in the cable shield and install another layer of copper braid or foil underneath the high- $\mu$  foil ungrounded at one end, producing a transfer impedance of 10 micro-ohm per meter, peak induced voltage to peak Waveform 4 current, with no saturation. The top layer of copper braid practically ensures no saturation of the high- $\mu$  foil.  
The designer must ensure that the circuits can withstand the common mode perturbation in the inner shield impedance at the ungrounded end, e.g. design in mode conversion control in the wiring and I/O circuits, transformer isolation, and/or adaptive software that detects the errant perturbation and cancels it out.

## 10. TEST PLANS

Figure 28 is a pictorial of a lab test set up for checking these theoretical models. The transfer impedance of several cable shields will be measured first as depicted in Figure 29. The plan is to perform this test with (1) a frequency sweep using a network analyzer and (2) a time domain Component A/Waveform 4 pulse and later, as much as possible, (3) saturate the high- $\mu$  foil shield with a higher current. In order to saturate the foil, the cable shield may have to be driven directly to obtain maximum current through it. An additional test will be run on the new cables to measure the effect of the open ended shield on differential swept frequency signals.

The tests are intended to (1) demonstrate how electrical currents divide between carbon and copper and (2) verify Schelkunoff's 74 year old theory of coaxial cable shielding.

The effects on the signals of the new layered cable shield with one end of the inner layer ungrounded will also be tested.

Rev. A: This test, as planned, is out of date with the new in-flight lightning interaction model. However, as soon as a new lightning test is designed that eliminates or minimizes the return current, this test set up will serve as a good model verification test for (1) the new in-flight lightning interaction producing only Waveform 4 instead of waveform 5A on the shields and (2) cable shielding characteristics.

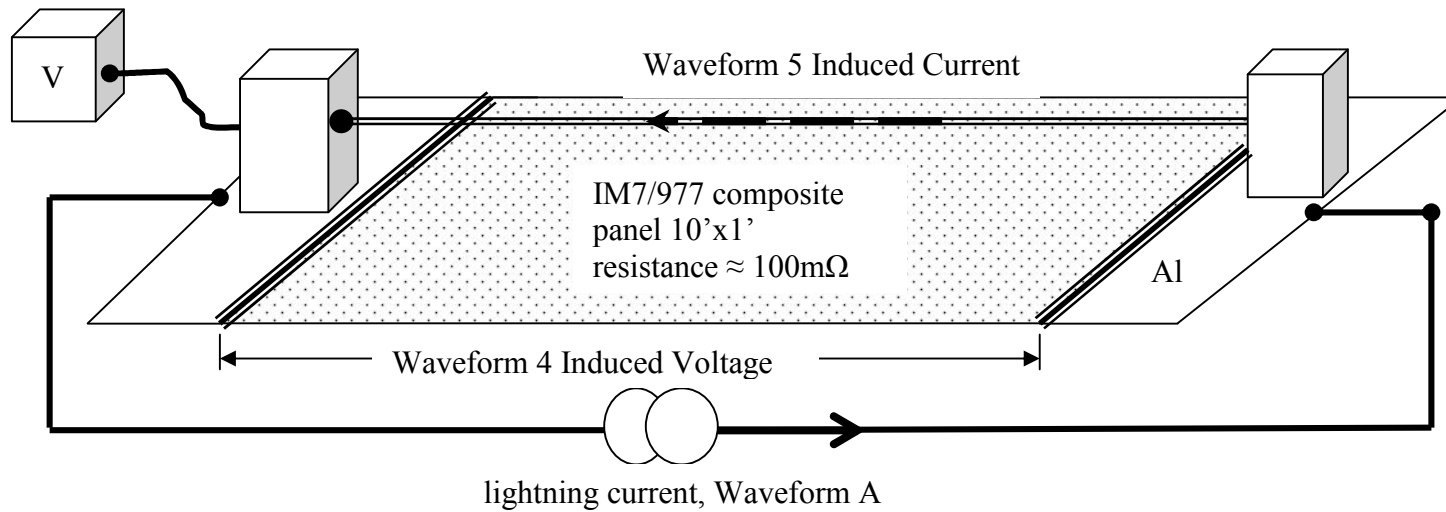


Figure 28. Indirect Lightning Test of Effect of Cable Shield on IR-Drop Induced Voltage and Waveform 5A Cable Current

28

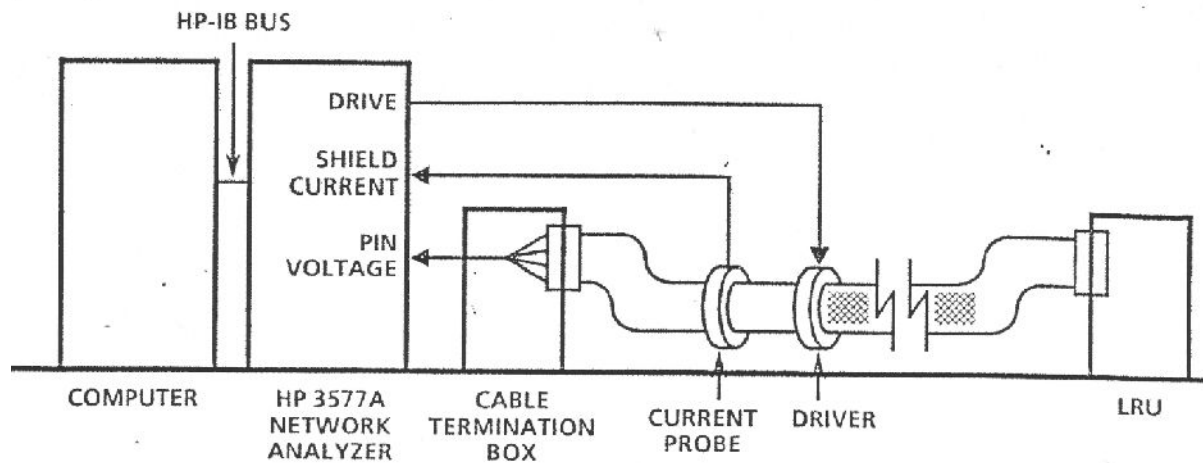


Figure 29. Cable Shield Transfer Impedance/Attenuation Test Method<sup>12</sup>

See Paper #4 Appendix B for a Simpler Method

Appendix A. Tycoelectronics/Raychem Spec Control Drawing<sup>11</sup>

SPECIFICATION CONTROL DRAWING			0024S0664
<b>CHEMINAX</b>	100 OHM, AWG 24, 19 STRANDS OF AWG 36, DATA BUS CABLE, EMP HARDENED, OPTIMIZED DOUBLE SHIELD, OUTER SPACE USE	Date	6-26-09
		Revision	Proposed 2
THIS SPECIFICATION SHEET FORMS A PART OF THE LATEST ISSUE OF RAYCHEM SPECIFICATION 1200.			
CONSTRUCTION DETAILS		ELECTRICAL CHARACTERISTICS	
<p><b>CONDUCTORS</b> AWG 24, 19 Strands of AWG 36, Silver-Coated High Strength Copper Alloy</p> <p><b>DIELECTRICS</b> Radiation-Crosslinked, Modified ETFE (Dual Extruded) Colors - Light Blue/White</p> <p><b>FILLERS</b> Radiation-Crosslinked, Modified ETFE</p> <p><b>1<sup>st</sup> SHIELD</b> AWG 38, Silver-Coated Copper Optimized</p> <p><b>1<sup>st</sup> JACKET</b> Radiation-Crosslinked, Modified ETFE Color - White</p> <p><b>WRAP</b> Mumetal Tape</p> <p><b>2<sup>nd</sup> SHIELD</b> AWG 38, Silver-Coated Copper Optimized</p> <p><b>2<sup>nd</sup> JACKET</b> Radiation-Crosslinked, Modified ETFE</p>		<p>CHARACTERISTIC IMPEDANCE 100 ± 5 ohms, Method C at 1 MHz</p> <p>MUTUAL CAPACITANCE 18.0 pF/ft. (nominal)</p> <p>ATTENUATION 1.4 dB/100 ft. (maximum) at 1 MHz</p> <p>SURFACE TRANSFER IMPEDANCE TBD (Per MIL-C-85485)</p>	
		<p><b>ADDITIONAL REQUIREMENTS</b></p> <p><b>COMPONENT WIRE PRIOR TO CABLING (Test Procedures per SAE A822768)</b></p> <p>CROSSLINK PROOF 300 ± 3°C for 1 hour, .750 inch mandrel, .625 lb., 2.5 kV dielectric test</p> <p>INSULATION (DIELECTRIC) (Total Insulation) ELONGATION 50% (minimum) TENSILE STRENGTH 5000 lbf/in<sup>2</sup> (minimum) INSULATION FLAWS SPARK TEST 3.0 kV (rms) IMPULSE TEST 8.0 kV (peak) INSULATION RESISTANCE 5000 megohms for 1000 ft. (minimum) LOW TEMPERATURE-COLD BEND -65 ± 3°C for 4 hours, .500 inch mandrel, 1.00 lb., 2.5 kV dielectric test SHRINKAGE 200 ± 3°C for 1 hour, .125 inch (maximum) in 12 inches</p> <p><b>FINISHED CABLE (Test Procedures per NEMA WC 27600, unless otherwise specified)</b></p> <p>BLOCKING 200°C for 6 hours</p> <p>CROSSLINKED VERIFICATION 300 ± 5°C for 6 hours, 6.00 inch mandrel</p> <p>FLAMMABILITY 3 seconds (maximum); 3 inches (maximum); (Method B of Spec 1200) no flaming of facial tissue</p> <p><b>JACKET</b></p> <p>ELONGATION 50% (minimum) TENSILE STRENGTH 5000 lbf/in<sup>2</sup> (minimum) JACKET FLAWS SPARK TEST 1.0 kV (rms) IMPULSE TEST 6.0 kV (peak) 1<sup>st</sup> JACKET THICKNESS .006 inch (nominal), .008 inch (maximum) 2<sup>nd</sup> JACKET THICKNESS .009 inch (nominal), .011 inch (maximum) LOW TEMPERATURE-COLD BEND -55 ± 5°C for 4 hours, 6.00 inch mandrel VOLTAGE WITHSTAND (DIELECTRIC) 1500 volts (rms) WRAP .002 inch thick (nominal) 25% overlap (minimum) WEIGHT 40.6 lbs/1000 ft. (nominal)</p> <p><b>OUTER SPACE REQUIREMENTS</b></p> <p>RADIATION RESISTANCE 500 megarads/6.25 inch mandrel 1.0 kV dielectric test</p> <p>VACUUM STABILITY TOTAL MASS LOSS (TML) 1.00% (maximum) VOLATILE CONDENSABLE MATERIAL (VCM) 0.10% (maximum) WEIGHT LOSS (Test per Spec 55): 0.45% (maximum)</p>	
<p>Outer jacket color will be white (designated by a "S" appended to the part number, e.g. 0024S0664-S) unless otherwise specified.</p> <p>Designate outer jacket color with a dash number in accordance with MIL-STD-681. Other codes and suffixes may be added to the part number, as necessary, to capture any additional requirements imposed by the purchase order.</p>			
<p>Users should evaluate the suitability of this product for their application. Specifications are subject to change without notice. Tyco Electronics also reserves the right to make changes in materials or processing, which do not affect compliance with any specification, without notification to Buyer.</p>			
Page 1 of 1	The TE logo, Tyco Electronics, Cheminax and Raychem are trademarks.		



Raychem Wire & Cable  
501 Oakside Avenue  
Redwood City, California 94063-3800  
1-800-227-8816 Fax: 1-650-381-6297

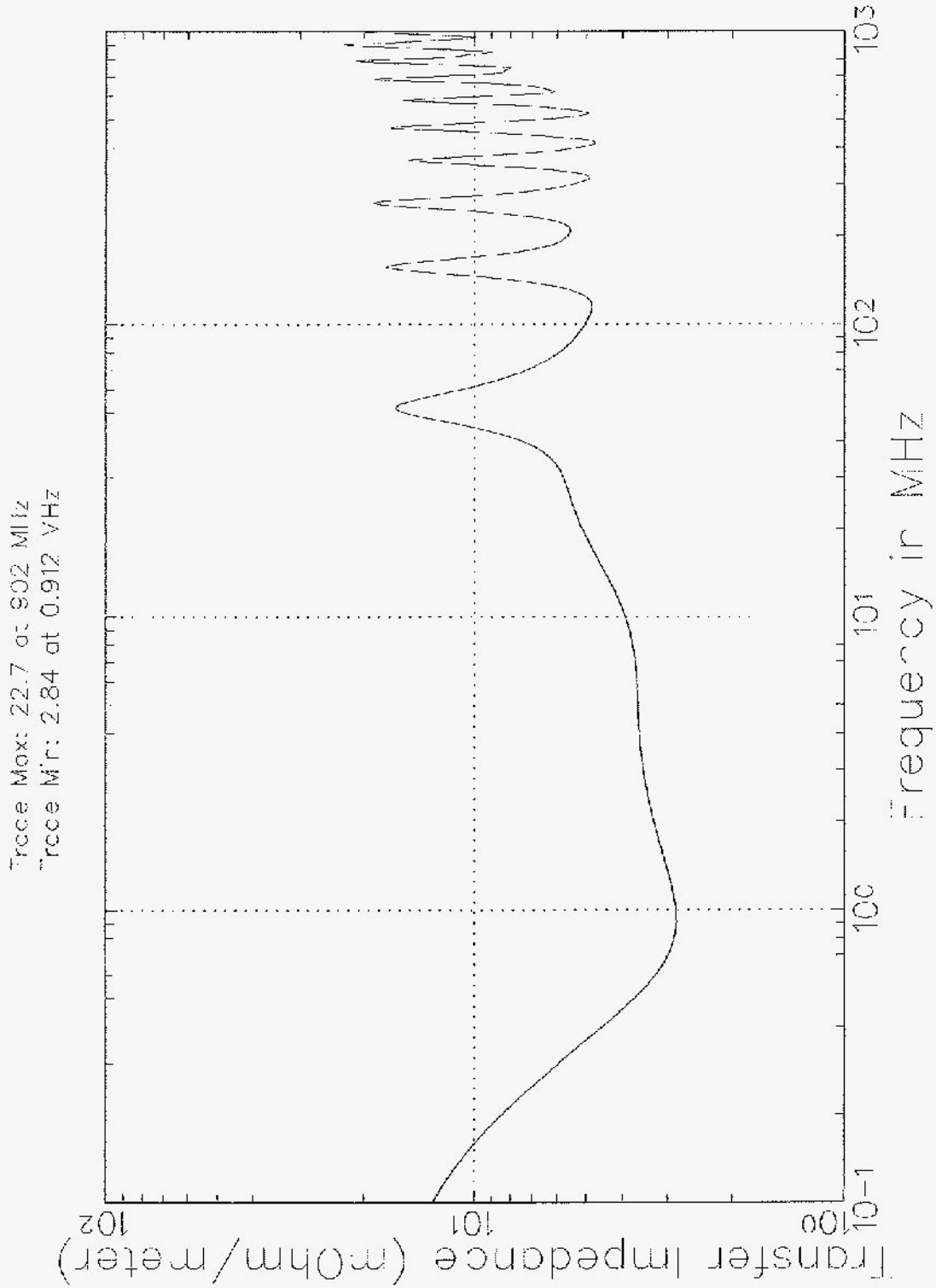
THIS SPECIFICATION SHEET TAKES PRECEDENCE OVER DOCUMENTS REFERENCED HEREIN. REFERENCED DOCUMENTS SHALL BE OF THE ISSUE IN EFFECT ON DATE OF INVITATION FOR BID.

Appendix B. Tycoelectronics/Raychem Transfer Impedance Data<sup>11</sup>

PRO-0024S0664-9  
1M

090029  
21C

DA0040/6 11/11/2009 Page 2



## REFERENCES

1. Schelkunoff, S. A., "The Electromagnetic Theory of Coaxial Transmission Lines and Cylindrical Shields", *The Bell System Technical Journal*, Volume XIII, 1934, 532-579
2. Lee, K. S. H., Editor, *EMP Interaction: Principles, Techniques, and Reference Data*, Taylor & Francis, NY, 1995, 505-510
3. Goldman, Stanford, *Laplace Transform Theory and Electrical Transients*, Dover Publications, Inc., NY, 1966
4. SAE ARP5412A, "Aircraft Lightning Environment and Related Test Waveforms", Society of Automotive Engineers, Aerospace Recommended Practice, PA, Revised 2005-02
5. SAE ARP5415A, "User's Manual for Certification of Aircraft Electrical/Electronic Systems for the Indirect Effects of Lightning", Society of Automotive Engineers, Aerospace Recommended Practice, PA, Revised 2002-04
6. RTCA/DO-160E, "Environmental Conditions and Test Procedures for Airborne Equipment", Section 22, Lightning Induced Transient Susceptibility and Section 23, Lightning Direct Effects, RTCA Inc., DC, December 9, 2004
7. Merewether, David E., "Analysis of Shielding Characteristics of Saturable Ferromagnetic Cable Shields", *IEEE Tran. EMC-12*, No. 3, August 1970, 134-137 (AFRL Interaction Note 67 on [www/unm.ecu.edu/summa/notes](http://www/unm.ecu.edu/summa/notes))
8. Merewether, David E., "Design of Shielded Cables using Saturable Ferromagnetic Materials", *IEEE Tran. EMC-12*, No. 3, August 1970, 138-141 (AFRL Interaction Note 68 on [www/unm.ecu.edu/summa/notes](http://www/unm.ecu.edu/summa/notes))
9. [http://raychem.tycoelectronics.com/datasheets/9-087\\_9-088\\_ElectrialShield.pdf](http://raychem.tycoelectronics.com/datasheets/9-087_9-088_ElectrialShield.pdf), Catalog 1654025, Revised 12-04, Miscellaneous, "Electrical Shielding"
10. ArcelorMittal, Denise, France, [www.imphy.com](http://www.imphy.com), brochure on Mumetal – Permphy & Superimphy, Fe-Ni Soft magnetic Alloys
11. Raychem private communication, July 2008, March 2011
12. William Prather, "Cable Shield Specifications and Measurement Techniques", Aircraft EMP Standards Meeting Defense Threat Reduction Agency, Air Force Research Laboratory, Directed Energy Directorate, 18 Oct 2006 [Techniques developed by Hoeft (BDM), Miller (TRW), & Prather.]
13. The Siemon Company private communication, 7/24/08, V. Maguire & D. Medeiros
14. Johnson & Graham, *High-Speed Signal Propagation*, Prentice Hall PTR, NJ, 2003
15. Texas Instruments Data Sheet, SLLS871, Nov 2007, for the AM26C31-EP Line Driver
16. Texas Instruments Data Sheet, SLLS870, Nov 2007, for the AM26C32-EP Line Receiver
17. Texas Instruments Data Sheet, SLLS428F, June 2000, Revised January 2004, TLK1501,

## 0.6 to 1.5 GBPS Transceiver

18. International Electrotechnical Commission Standard IEC 61076-3-104 Ed2

19. [http://www.maxim-ic.com/appnotes.cfm/an\\_pk/2116](http://www.maxim-ic.com/appnotes.cfm/an_pk/2116), MAX1480A, B, Complete, Isolated RS-485/RS-422 Data Interface

20. <http://www.analog.com/en/interface/digital-isolators/ADUM1200/products/product.html>, ADUM1200: Dual-Channel Digital Isolator (2/0 Channel Directionality)

21. 10/100 Base-T Single Port Transformer Modules, Pulse Engineering, Inc., [http://www.datasheetcatalog.org/datasheets2/19/194306\\_1.pdf](http://www.datasheetcatalog.org/datasheets2/19/194306_1.pdf)  
(These have center-tapped transformers, bifilar chokes, and common mode filtering.)

22. Raychem Specification Control Drawing, EPD-RWC-21824 (courtesy of Robert Moore.)

23. West, Larry, "In-Flight vs. Ground-Test Lightning Interactions in Composite Airframes, Effects of External vs. Internal inductance, An Errata to Everything Previously Published," IN615, April 2011

24. West, Larry, "Allocating Indirect Lightning to Cables & Boxes at Program Inception, Application of Ohm's Law, Kirchhoff's Laws, Faraday's Law & Scaling by Geometric, Electrical, & Spectral Parameters", paper #3, April 2011

25. West, Larry & Norgard, John, "In-Flight vs. Ground-Test Lightning Interactions in Composite Aircraft", IEEE AP-S/URSI Spokane, July 2011

26. West, Larry, "Lightning Induced Waveforms 4 and 5A in Composite Airframes, The Inability of Copper Braid to Shield It, and A New Layered Copper Braid and High- $\mu$  Foil Shield", Interaction Note 608, February 2009

27. West, Larry, *Indirect Lightning in Composite Aircraft*, Self Published Public Domain, TX, 2011